

Search for physics beyond the standard model in events with τ leptons, jets, and large transverse momentum imbalance in pp collisions at $\sqrt{s} = 7$ TeV

The CMS Collaboration*

CERN, Geneva, Switzerland

Received: 16 January 2013 / Revised: 11 June 2013 / Published online: 16 July 2013

© CERN for the benefit of the CMS collaboration 2013. This article is published with open access at Springerlink.com

Abstract A search for physics beyond the standard model is performed with events having one or more hadronically decaying τ leptons, highly energetic jets, and large transverse momentum imbalance. The data sample corresponds to an integrated luminosity of 4.98 fb^{-1} of proton-proton collisions at $\sqrt{s} = 7$ TeV collected with the CMS detector at the LHC in 2011. The number of observed events is consistent with predictions for standard model processes. Lower limits on the mass of the gluino in supersymmetric models are determined.

1 Introduction

The standard model (SM) of particle physics has been successful in explaining a wide variety of data. In spite of this, the SM is incomplete. For example, it possesses a divergence in the Higgs sector [1] and has no cold dark matter (DM) candidate [2]. Many models of physics beyond the SM (BSM) have been proposed in order to address these problems.

DM particles, if produced in proton-proton collisions at the CERN Large Hadron Collider (LHC), would escape detection and result in a significant transverse momentum (p_T) imbalance in the detector. Additionally, cascade decays of heavy colored particles to final states with a high multiplicity of energetic jets and τ leptons appear very naturally in many BSM physics scenarios. Hence, events with multiple τ lepton candidates, large jet multiplicity, and significant transverse momentum imbalance, represent a distinct signature of new physics. In this paper, focus is placed on final states with hadronically decaying τ leptons. In what follows, the visible part of a hadronically decaying τ lepton will be referred to as τ_h .

In certain models of supersymmetry (SUSY), the lightest supersymmetric particle (LSP) is a candidate for DM. It has been appreciated for some time that the DM relic density may be sensitive to coannihilation processes involving the LSP and the next-to-lightest supersymmetric particle (NLSP). Coannihilation is characterized by a mass difference (ΔM) between the NLSP and the LSP of approximately 5–15 GeV [3–6]. This small mass difference would be necessary to allow the NLSP to coannihilate with the LSP in the early universe, leading to the dark matter abundance that is currently observed [7]. If the supersymmetric partner of the τ lepton, the stau ($\tilde{\tau}$), is the NLSP, and if the $\tilde{\tau}$ decays primarily to a τ lepton and the LSP, small values of ΔM would lead to final states with low-energy τ leptons ($p_T \sim \Delta M$) [8]. Decays of colored SUSY particles can produce the $\tilde{\tau}$ via chargino ($\tilde{\chi}^\pm$) or neutralino ($\tilde{\chi}^0$) intermediate states (e.g., $\tilde{\chi}_2^0 \rightarrow \tau \tilde{\tau} \rightarrow \tau \tau \tilde{\chi}_1^0$), resulting in final states with at least one τ_h .

We present a search for BSM particles in events with exactly one τ_h lepton and jets (single- τ_h final state), and in events with jets and two or more τ_h leptons (multiple- τ_h final state). These two topologies provide complementary sensitivity to models with a wide range of ΔM values. For example, in the case of very small values of ΔM (~ 5 GeV), the low-energy τ_h cannot be effectively detected and the search for new physics in the single- τ_h final state has better sensitivity. The analysis is performed using proton-proton collision data at $\sqrt{s} = 7$ TeV collected with the Compact Muon Solenoid (CMS) detector [9] at the LHC in 2011. The data sample corresponds to an integrated luminosity of $4.98 \pm 0.11 \text{ fb}^{-1}$. The search is characterized by methods that determine the backgrounds directly from data, to reduce the reliance on simulation. To illustrate the sensitivity of this search to BSM processes, the constrained minimal supersymmetric extension of the standard model, or minimal supergravity, is chosen as the benchmark [3, 10, 11]; we

* e-mail: cms-publication-committee-chair@cern.ch

denote this benchmark as “CMSSM”. An interpretation of the results in the context of simplified model spectra (SMS) [12, 13] is also presented. The ATLAS collaboration has published a result on a search for one or more hadronically decaying tau leptons, highly energetic jets, and a large transverse momentum imbalance probing minimal Gauge Mediated Symmetry Breaking (GMSB) models [14].

2 The CMS detector

The central feature of the CMS apparatus is a superconducting solenoid, of 6 m inner diameter, providing a magnetic field of 3.8 T. Within the field volume are a silicon pixel and strip tracker, a crystal electromagnetic calorimeter (ECAL), which includes a silicon sensor preshower detector in front of the ECAL endcaps, and a brass-scintillator hadron calorimeter. Muons are measured in gas-ionization detectors embedded in the steel return yoke. In addition to the barrel and endcap detectors, CMS has extensive forward calorimetry.

The inner tracker measures charged particles within $|\eta| < 2.5$ and provides an impact parameter resolution of about 15 μm and a p_{T} resolution of about 1.5 % for 100 GeV particles. Collision events are selected with a first-level trigger based on fast electronics, and a higher-level trigger that runs a version of the offline reconstruction program optimized for speed.

The CMS experiment uses a right-handed coordinate system, with the origin at the nominal interaction point, the x axis pointing to the center of the LHC ring, the y axis pointing up (perpendicular to the plane of the LHC ring), and the z axis along the counterclockwise beam direction. The polar angle θ is measured from the positive z axis and the azimuthal angle in the x - y plane. The pseudorapidity is given by $\eta = -\ln[\tan(\theta/2)]$.

3 Object reconstruction and identification

Jets in the detector are reconstructed using particle-flow (PF) objects [15]. In the PF approach, information from all subdetectors is combined to reconstruct and identify final-state particles (muons, electrons, photons, and charged and neutral hadrons) produced in the collision. The anti- k_{T} clustering algorithm [16] with a distance parameter $R = 0.5$ is used for jet clustering. Jets are required to satisfy criteria designed to identify anomalous behavior in the calorimeters, and to be well separated from any identified τ lepton.

Validation and efficiency studies are performed utilizing events with a τ_h lepton and a light-lepton ℓ , with ℓ representing an electron (e) or muon (μ). Muons are reconstructed using the tracker and muon chambers. Selection requirements based on the minimum number of hits in the silicon tracker, pixel detector, and muon chambers are applied

to suppress muon backgrounds from decays-in-flight of pions or kaons [17]. Electrons are reconstructed by combining tracks with ECAL clusters. Requirements are imposed to distinguish between prompt and non-prompt electrons, where the latter can arise from charged pion decay or photon conversion [18]. The light-lepton candidates are required to satisfy both track and ECAL isolation requirements. The track isolation variable is defined as the sum of the p_{T} of the tracks, as measured by the tracking system, within an isolation cone of radius $\Delta R = \sqrt{(\Delta\eta)^2 + (\Delta\phi)^2} = 0.4$ centered on the light-lepton track. The ECAL isolation variable is based on the amount of energy deposited in the ECAL within the same isolation cone. In both cases the contribution from the light-lepton candidate is removed from the sum.

Reconstruction of hadronically decaying τ leptons is performed using the hadron-plus-strips (HPS) algorithm [19], designed to optimize the performance of τ_h reconstruction by considering specific τ_h decay modes. To suppress backgrounds in which light-quark or gluon jets mimic hadronic τ decays, a τ_h candidate is required to be spatially isolated from other energy deposits in the calorimeter. Charged hadrons and photons not considered in the reconstruction of the τ_h decay mode are used to calculate the isolation. Additionally, τ_h candidates are required to be distinguished from electrons and muons in the event. In this analysis, two HPS isolation definitions are used. The τ_h isolation definition used for single- τ_h final states rejects a τ_h candidate if one or more charged hadrons with $p_{\text{T}} > 1.0$ GeV or one or more photons with transverse energy $E_{\text{T}} > 1.5$ GeV is found within an isolation cone of radius $\Delta R = 0.5$. The τ_h isolation definition used for multiple- τ_h final states rejects a τ_h candidate if one or more charged hadrons with $p_{\text{T}} > 1.5$ GeV or one or more photons with transverse energy $E_{\text{T}} > 2.0$ GeV is found within an isolation cone of radius $\Delta R = 0.3$. The isolation criteria used for the multiple- τ_h final state increases the signal-to-background ratio while reducing the rate of τ_h misidentification. This affects the yield of events with light-quark or gluon jets that are misidentified as τ_h leptons, which depends on the square of the misidentification rate. Here a final state with exactly two τ_h candidates is considered since events with more than two τ_h candidates are only a small fraction (< 1 %) of events.

The missing transverse momentum \cancel{p}_{T} is defined as:

$$\cancel{p}_{\text{T}} = \left| \sum \mathbf{p}_{\text{T}}^{\text{jet}} \right|, \quad (1)$$

where the sum runs over all the jets with $p_{\text{T}}^{\text{jet}} > 30$ GeV inside the fiducial detector volume of $|\eta| < 5$. The vector \cancel{p}_{T} is the negative of the vector sum in Eq. (1). The observable $H_{\text{T}} = \sum \mathbf{p}_{\text{T}}^{\text{jet}}$ is used to estimate the overall energy scale of the event. For the single- τ_h final state, H_{T} is calculated using jets with $p_{\text{T}} > 50$ GeV and will be referred to as H_{T}^{50} . For

the multiple- τ_h final state, H_T is calculated using jets with $p_T > 30$ GeV and will be referred to as H_T^{30} . In both instances of the H_T calculation, we consider all jets in $|\eta| < 5$ (the fiducial detector limit). The use of a lower p_T threshold for the jets in the multiple- τ_h final state increases the efficiency of signal events without significantly increasing the background.

4 Signal and background samples

The major sources of SM background are top-quark pair ($t\bar{t}$) events and events with a W or Z boson accompanied by jets. Both $t\bar{t}$ and W + jets events can have genuine τ_h leptons, large genuine \cancel{H}_T from W boson decays, and jets that can be misidentified as a τ_h . Similarly, Z + jets events with $Z(\rightarrow \nu\nu)$ and with one or more jets misidentified as a τ_h lepton provide a source of background. Z + jets events with $Z(\rightarrow \nu\nu)$ present a background because of the genuine τ_h leptons and the genuine \cancel{H}_T from the neutrinos in the τ_h decay. QCD multijet events can become a background when a mismeasured jet gives rise to large \cancel{H}_T and jets are misidentified as τ_h leptons.

Data are compared with predictions obtained from samples of Monte Carlo (MC) simulated events. Signal and background MC samples are produced with the PYTHIA 6.4.22 [20] and MADGRAPH [21] generators using the Z2 tune [22] and the NLO CTEQ6L1 parton distribution function (PDF) set [23]. The τ lepton decays are simulated with the TAUOLA [24] program. The generated events are processed with a detailed simulation of the CMS apparatus using the GEANT4 package [25]. The MC yields are normalized to the integrated luminosity of the data using next-to-leading order (NLO) cross sections [26–31]. For the 2011 LHC running conditions, the mean number of interactions in a single beam crossing is ~ 10 . The effect of multiple interactions per bunch crossing (pileup) is taken into account by superimposing MC minimum-bias events so that the probability distribution for overlapping pp collisions in the simulation matches the measured distribution.

5 Event selection

Events for both the single- and multiple- τ_h final states are selected using a trigger that requires $\cancel{H}_T > 150$ GeV. This trigger allows us to maintain sensitivity in regions where the p_T value of the τ_h is small ($p_T \sim 15$ GeV). This trigger efficiency, for an offline selection requirement of $\cancel{H}_T > 250$ GeV, is 98.9 %. For the τ_h efficiency and validation studies, samples are chosen using triggers that require the presence of both a τ_h candidate and a muon.

The τ_h candidates must satisfy $p_T > 15$ GeV and $|\eta| < 2.1$. For the single- τ_h final state we require that no additional

light leptons be present in the event. This requirement suppresses background from $t\bar{t}$, W + jets, and Z + jets events. For the multiple- τ_h final state there is no requirement placed on the number of light leptons.

For the single- τ_h final state, we define a baseline event selection $H_T^{50} > 350$ GeV and $\cancel{H}_T > 250$ GeV. The sample obtained with the baseline selection is used to validate the background predictions. The signal region (SR) for the single- τ_h final state is defined by $H_T^{50} > 600$ GeV and $\cancel{H}_T > 400$ GeV.

For the multiple- τ_h final state, the SR is defined by $\cancel{H}_T > 250$ GeV and by the requirement that there be at least two jets with $p_T > 100$ GeV and $|\eta| < 3.0$. QCD multijet events are rejected by requiring the azimuthal difference $\Delta\phi(j_2, \cancel{H}_T)$ between the second leading jet in p_T and \cancel{H}_T to satisfy $|\Delta\phi(j_2, \cancel{H}_T)| > 0.5$. Finally, events are required to contain at least one $\tau_h\tau_h$ pair separated by $\Delta R(\tau_{h,i}, \tau_{h,j}) > 0.3$.

6 Background estimate

The background contributions are categorized differently for the single- and multiple- τ_h final states. For the single- τ_h final state, the background contributions are divided into events containing a genuine τ_h and events where a jet is misidentified as a τ_h . For the multiple- τ_h final state, the main background contribution arises from misidentified τ_h leptons. We identify the different sources of background individually using dedicated data control regions (CR).

6.1 Estimate of backgrounds in the single- τ_h final state

In the single- τ_h final state, the largest background contribution comes from W + jets events that contain a genuine τ_h lepton. The other significant contribution arises from QCD multijet events in which a jet is misidentified as a τ_h . The W + jets background contribution is estimated using a sample of W + jets events with $W \rightarrow \mu\nu$. The QCD multijet background is determined by selecting a QCD-dominated CR and evaluating the τ_h misidentification rate.

6.1.1 Estimate of the W + jets background in the single- τ_h final state

To evaluate the W + jets background, we exploit the similarity between W decays to a muon and to a tau lepton and select a sample of W + jets events with $W(\rightarrow \mu\nu)$. This sample will be referred to as the muon control sample. To select the muon control sample, events are required to contain exactly one muon and no reconstructed τ_h or electron. To emulate the τ_h acceptance, the muon is required to satisfy $|\eta| < 2.1$. The yields in the muon control sample are

corrected for muon reconstruction ($\varepsilon_\mu^{\text{reco}}$) and isolation efficiency ($\varepsilon_\mu^{\text{iso}}$). The muon reconstruction efficiency is derived from data using a sample of $Z + \text{jets}$ events and parameterized as a function of p_T and η . The muon isolation criteria help to distinguish between muons from the decay of the W boson and muons from semileptonic decays of c and b quarks. The isolation efficiency is parameterized as a function of the separation from the nearest jet and the momentum of the jet. A correction factor (P_μ^W) is applied to the muons in the muon control sample to account for muons that do not come from a τ -lepton decay. This correction factor depends on the p_T of the muon and the $\#_T$ value in the event and is derived from a simulated sample of $W + \text{jets}$ events.

As the muons in the muon control sample are selected to mimic a τ_h , a correction is applied to emulate the probability to reconstruct and identify a τ_h lepton. The reconstruction and identification efficiency $\varepsilon_\tau^{\text{reco}}$ is parameterized as a function of the p_T of the τ_h candidate and as a function of the total number N of charged particles and photons in the isolation cone [Fig. 1(a)]. Corrections are also applied to account for the hadronic branching fraction ($f_\tau^{\text{bf(hadr)}}$) of a τ lepton. Except for the $f_\tau^{\text{bf(hadr)}}$ the values of the correction factors differ in each event. The corrections are combined to define an overall event weight, defined as:

$$f_{\text{event}}^{\text{corr}} = \frac{P_\mu^W \times \varepsilon_\tau^{\text{reco}} \times f_\tau^{\text{bf(hadr)}}}{\varepsilon_\mu^{\text{reco}} \times \varepsilon_\mu^{\text{iso}}} \quad (2)$$

A τ_h response template is derived from simulated events. The response template is given by the ratio of the reconstructed energy of the τ_h to the true generator-level energy. The τ_h response depends on the transverse momentum of the generated τ lepton [Fig. 1(b)] and on the number of reconstructed primary vertices in the event. The muon p_T spectrum is smeared as a function of p_T and the number of primary vertices to mimic the p_T distribution of the τ_h .

Fully simulated $W + \text{jets}$ events are used to verify the procedure. Figure 2 shows the H_T^{50} and $\#_T$ distributions from simulated $W + \text{jets}$ events for the single- τ_h final state. These events satisfy the baseline selection described in Sect. 5. The reconstructed τ_h is required to match a hadronically decaying generated tau lepton, to ensure that only the genuine tau background is addressed in this check. The event yield and distributions are compared with the prediction from the simulated muon control sample and agree within statistical uncertainties, thus verifying the closure of the method in MC simulation. Hence, the predicted H_T^{50} and $\#_T$ distributions from the muon control sample can be taken to describe a τ_h sample within statistical uncertainties.

The muon control sample consists primarily of $W + \text{jets}$ events, but also contains $t\bar{t}$ events in which one W boson decays into a muon while the other W boson decays either into an unidentified τ lepton or into a light lepton that

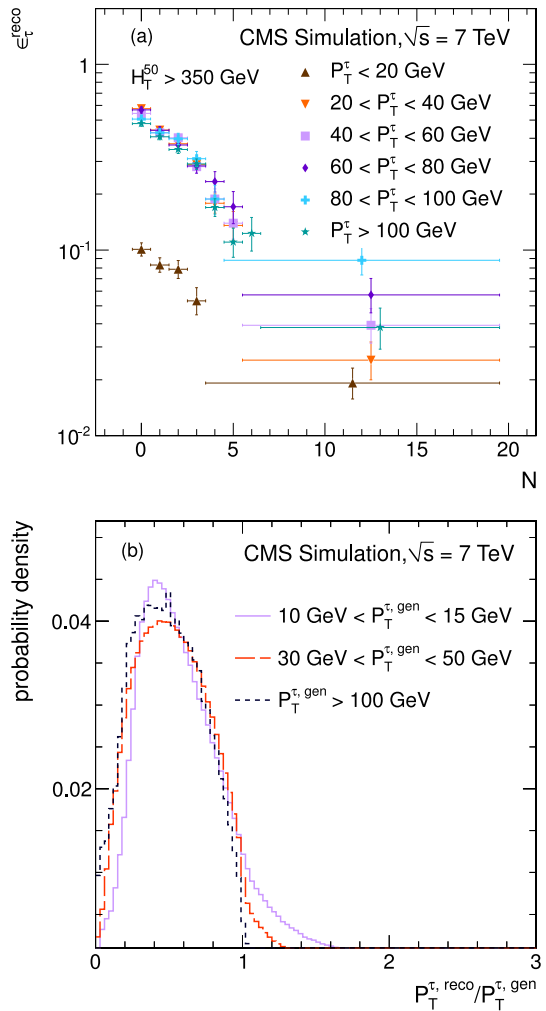


Fig. 1 (a) Dependence of the τ_h reconstruction efficiency $\varepsilon_\tau^{\text{reco}}$ on the number of additional particles N in the isolation cone in bins of τ_h lepton p_T for the single- τ_h final state, where N is the total number of the photons and charged hadrons in the isolation cone, and (b) dependence of τ_h response on $p_{\tau, \text{gen}}^\tau$. Both distributions are derived from a simulated sample of $W(\rightarrow \tau\nu) + \text{jets}$ events

is not reconstructed. Any isolated muons produced through the decay of b or c quarks can also contribute to the muon control sample. SM processes containing a Z boson or two W bosons can also contribute to the muon control sample if one of the two decay muons is not reconstructed.

The true event yields of each process as determined from simulation are summarized in Table 1 for the baseline and SR selections. For both selections the number of predicted events with a genuine τ_h lepton is seen to agree with the true number of events. The value of $\varepsilon_\tau^{\text{reco}}$ that is used to calculate the predicted rate is measured in a sample of $W + \text{jets}$ and is different from the value that would be measured in a sample of $t\bar{t}$ events. This leads to an overestimation of the $t\bar{t}$ contribution. A systematic uncertainty is assigned to account for this overestimation.

Table 1 The selected and predicted background contributions for simulated events with a genuine τ_h passing the baseline and signal selection in the single- τ_h final state. The reconstructed τ_h is required to

$L = 4.98 \text{ fb}^{-1}$	Baseline selection		Signal selection	
	Selected	Predicted	Selected	Predicted
$W(\rightarrow \ell\nu) + \text{jets}$	452 ± 30	441 ± 21	28.9 ± 7.5	34.9 ± 5.9
$t\bar{t}$	60.6 ± 3.7	63.2 ± 2.1	1.6 ± 0.6	2.9 ± 0.4
$Z(\rightarrow \ell\ell) + \text{jets}$	10.9 ± 2.1	8.4 ± 1.3	0.8 ± 0.6	0.4 ± 0.3
W^+W^-	15.1 ± 1.6	14.4 ± 1.1	0.5 ± 0.3	1.3 ± 0.3
Sum	539 ± 30	527 ± 21	31.8 ± 7.5	39.5 ± 5.9

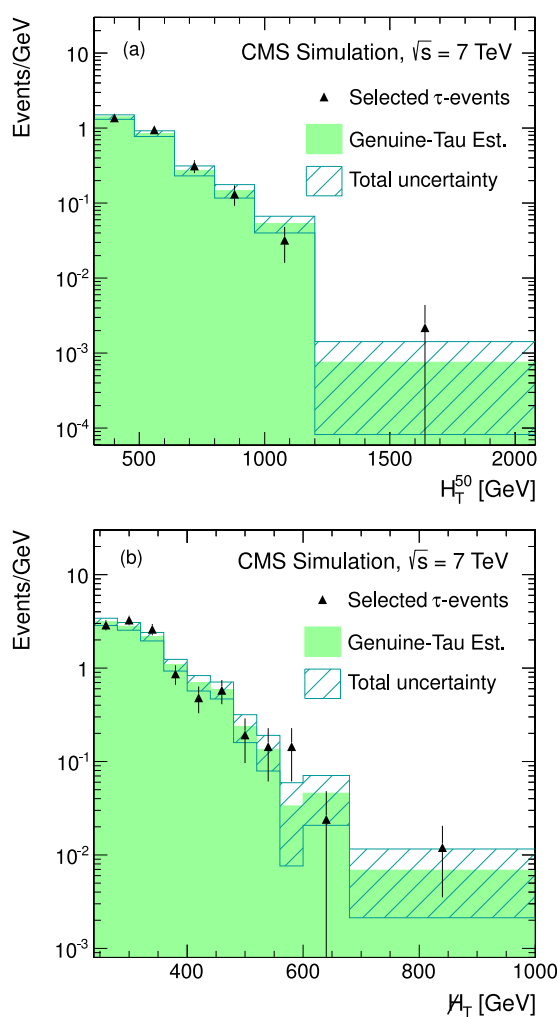


Fig. 2 Distributions of (a) H_T^{50} and (b) H_T for the genuine τ_h estimate in simulated $W + \text{jets}$ events for the single- τ_h final state. The black triangles show the results for events that satisfy the baseline selection and that contain a reconstructed τ_h matched to the visible part of a generated, hadronically decaying τ lepton. The filled green areas show the prediction obtained from the simulated muon control sample. The hatched areas are the total uncertainty on the prediction (Color figure online)

match the visible part of the generated, hadronically decaying τ -lepton. The predictions are derived from the muon control sample

6.1.2 Estimate of the QCD multijet background in the single- τ_h final state

To estimate the background where a jet is misidentified as a τ_h lepton, a QCD-dominated control sample is obtained by selecting events with $H_T^{50} > 350 \text{ GeV}$ and $40 < \cancel{H}_T < 60 \text{ GeV}$. The control sample is selected using a prescaled H_T trigger with criteria that lead to a sample where about 99 % of the events arise from QCD multijet production. The probability for a jet to be misidentified as a τ_h lepton is measured by determining the fraction of jets from the single- τ_h control sample that pass the τ_h identification criteria. Jets considered in the calculation of the misidentification rate satisfy the requirements $p_T > 5 \text{ GeV}$ and $|\eta| < 2.5$. The misidentification rates f_i for each jet i depend on η and p_T and are used to determine an overall weight, which is applied to each event. The event weights are defined as:

$$w_{\text{event}}^{\text{corr}} = 1 - \prod_i^n (1 - f_i), \quad (3)$$

where n is the number of jets. The measured misidentification rates shown in Fig. 3(a) are applied to data events in the region with $H_T^{50} > 350 \text{ GeV}$ and with $H_T^{50} > 600$ for two regions of \cancel{H}_T : $60 < \cancel{H}_T < 80 \text{ GeV}$ and $80 < \cancel{H}_T < 100 \text{ GeV}$. These four regions are dominated by QCD multijet events. The results for data and simulation, as well as the predicted fraction of QCD multijet events, are shown in Table 2. The ratio of selected events over predicted events is statistically compatible with one and stable over the range of \cancel{H}_T . Figure 3(b) shows the \cancel{H}_T distributions of predicted and selected events for simulated QCD multijet events with $H_T^{50} > 350 \text{ GeV}$. The two distributions agree over the whole range of \cancel{H}_T .

6.2 Estimate of backgrounds in the multiple- τ_h final state

The estimate of the SM background contributions to the SR sample for multiple- τ_h events is based on the number of observed events in CRs. The events in each CR are selected

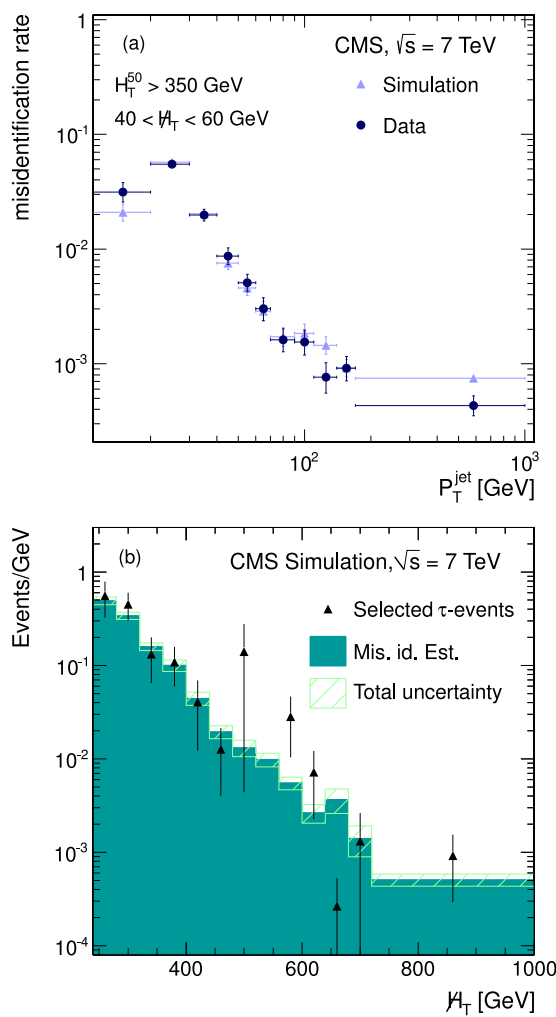


Fig. 3 (a) The rate of jet misidentification as a τ_h lepton in simulation (triangular symbols) and data (circular symbols) as a function of p_T^{jet} for events with $H_T^{50} > 350 \text{ GeV}$ and $40 < H_T < 60 \text{ GeV}$; (b) The $\#H_T$ distribution estimated in simulated events with $H_T^{50} > 350 \text{ GeV}$, where the triangular symbols represent events that pass the baseline selection, the filled blue area shows the predicted events, and the hatched area shows the total uncertainty on the prediction. These distributions correspond to the single- τ_h final state (Color figure online)

with similar selection requirements to those used in the SR, but are enriched with events from the background process in question. Correction factors and selection efficiencies are measured in those CRs and used to extrapolate to the SR. We use the observed jet multiplicity in each CR along with the measured rate at which a jet is misidentified as a τ_h to calculate the yield in the SR. The following equation is used to estimate each background contribution B:

$$N_B^{\text{SR}} = N_B^{\text{CR}} [\alpha_{\tau\tau} \mathcal{P}(0) + \alpha_{\tau j} \mathcal{P}(1) + \alpha_{jj} \mathcal{P}(2)], \quad (4)$$

where N_B^{SR} is the predicted rate in the SR, N_B^{CR} is the observed number of events in the CR, and α_{xy} is the correction factor for acceptance and efficiency for events in the

Table 2 The percentage of QCD multijet events in the $\#H_T$ binned samples for different QCD multijet dominated regions in the single- τ_h final state

$H_T^{50} > 350 \text{ GeV}$	$\#H_T$ [GeV]		
	60–80	80–100	>250
QCD fraction	97 %	93 %	6 %
selected/predicted (sim)	0.98 ± 0.06	0.96 ± 0.07	1.24 ± 0.28
selected/predicted (data)	1.01 ± 0.08	0.88 ± 0.13	–
$H_T^{50} > 600 \text{ GeV}$			>400
QCD fraction	96 %	93 %	17 %
selected/predicted (sim)	0.94 ± 0.09	0.85 ± 0.09	2.43 ± 1.45
selected/predicted (data)	1.14 ± 0.26	0.97 ± 0.37	–

CR with true physics objects “x” and “y”. Here the physics object can be a τ_h or a quark or gluon jet. Since the dominant SM backgrounds contribute to the SR when jets are misidentified as τ_h lepton, the background estimation strategy outlined in Eq. (4) relies on the determination of the event probability $\mathcal{P}(m)$ for at least “m” jets to be misidentified as a τ_h , where $\mathcal{P}(m)$ is the product of three factors: (i) the probability $P(N)$ for an event to contain N jets, (ii) the number of possible ways for exactly n jets to pass the τ_h identification criteria given N possible jets $C(N, n) = N!/n!(N - n)!$, and (iii) the probability f for a single jet to be misidentified as a τ_h . The $\mathcal{P}(m)$ terms are given by:

$$\mathcal{P}(m) = \sum_{N=m}^{\infty} P(N) \sum_{n=m}^N C(N, n) f^n (1-f)^{N-n}. \quad (5)$$

Equation (5) would be identical to Eq. (3) if used in the case of the single- τ_h final state. Equation (4) is used to estimate the $t\bar{t}$, $W + \text{jets}$, and $Z + \text{jets}$ background contributions to the SR. The $P(N)$ terms are determined from data using the jet multiplicity distribution in each CR, while the f terms are measured for each background process by determining the fraction of jets in each CR that pass the τ_h identification criteria. Since the QCD multijet contribution to the SR for the multiple- τ_h final state is negligible according to simulation, a data-to-MC scale factor is used to correct the QCD multijet prediction from simulation. In the sections that follow, the selections used to define high purity CRs are outlined and the correction factors α_{xy} used in Eq. (4) are defined. The fraction of events with two τ_h leptons is denoted $A_{\tau\tau}$, the fraction with one τ_h lepton and one jet misidentified as a τ_h lepton is denoted $A_{\tau j}$, and the fraction with two jets misidentified as τ_h leptons is denoted A_{jj} .

6.2.1 Estimate of the $t\bar{t}$ event background to the multiple- τ_h final state

To estimate the contribution of $t\bar{t}$ events to the multiple- τ_h SR, a CR is selected by removing the τ_h isolation re-

quirement and by requiring the presence of at least two b-quark jets (b jets), identified using the track-counting-high-efficiency (TCHE) algorithm at the medium working point [32]. Because QCD multijet, $W + \text{jets}$, $Z(\rightarrow \tau\tau) + \text{jets}$ and $Z(\rightarrow \nu\nu) + \text{jets}$ events are unlikely to contain two b jets, this requirement provides a sample in which about 99 % of the events are $t\bar{t}$ events, according to simulation. Figure 4(a) shows the p_T distribution of τ_h leptons in the $t\bar{t}$ CR for data and simulation.

According to simulation, the fraction of events in the $t\bar{t}$ control sample that contains one genuine τ_h is $A_{\tau j} = 0.166 \pm 0.011$, while the fraction without a genuine τ_h is $A_{jj} = 0.834 \pm 0.025$. The genuine $\tau_h\tau_h$ contribution is negligible ($A_{\tau\tau} \sim 0$) according to simulation. Incomplete knowledge of the genuine $\tau_h\tau_h$ contribution is included as a source of systematic uncertainty in the $t\bar{t}$ background prediction. Therefore, $\alpha_{\tau j}$ in Eq. (4) is given by $A_{\tau j}\varepsilon_\tau^{\text{iso}}/P(2 \text{ b jets})$, where $\varepsilon_\tau^{\text{iso}}$ is the probability for a τ_h lepton to pass the isolation requirement, while α_{jj} is given by $A_{jj}/P(2 \text{ b jets})$. The probability $P(2 \text{ b jets})$ to identify two or more b jets is determined by the b jet identification efficiency factor [32]. The number of $t\bar{t}$ events in the SR is calculated as:

$$N_{t\bar{t}}^{\text{SR}} = \frac{N_{t\bar{t}}^{\text{CR}}}{P(2 \text{ b jets})} [A_{\tau j}\varepsilon_\tau^{\text{iso}}\mathcal{P}(1) + A_{jj}\mathcal{P}(2)]. \quad (6)$$

The probability for a jet in a $t\bar{t}$ event to be misidentified as a τ_h lepton has an average measured value of $f = 0.022 \pm 0.004$. Cross checks are made to validate the use of the b-jet identification efficiency as measured in Ref. [32] for this analysis. The estimated $t\bar{t}$ contribution in the SR is determined to be $N_{t\bar{t}}^{\text{SR}} = 2.03 \pm 0.36$.

6.2.2 Estimate of the $Z(\rightarrow \nu\nu) + \text{jets}$ event background to the multiple- τ_h final state

The contribution of $Z(\rightarrow \nu\nu) + \text{jets}$ events to the multiple- τ_h SR is evaluated by selecting a sample of $Z(\rightarrow \mu\mu) + \text{jets}$ events and treating the muons as neutrinos. The sample is collected using a trigger designed to select a muon and a τ_h . Jet selection criteria similar to those used for the SR sample are imposed. In addition, we require two muons passing the criteria outlined in Sect. 3. The control sample has a purity of about 99 % as estimated from simulation. The $\#_T$ distribution for events in this CR is shown in Fig. 4(b). The $Z(\rightarrow \nu\nu) + \text{jets}$ background is estimated by interpreting the p_T of the pair of muons as $\#_T$. In order to predict the $Z(\rightarrow \nu\nu) + \text{jets}$ rate in the SR, the $Z(\rightarrow \mu\mu) + \text{jets}$ sample is corrected for the ratio of the branching fractions $R = B(Z \rightarrow \nu\nu)/B(Z \rightarrow \mu\mu)$, for trigger efficiencies, for the geometric acceptance A_μ as measured from simulation, and for the reconstruction efficiency

$\varepsilon_\mu^{\text{reco}}$ as measured from data. Therefore, α_{jj} in Eq. (4) is given by:

$$\frac{1}{A_\mu^2\varepsilon_\mu^{\text{reco}2}} \frac{B(Z \rightarrow \nu\nu)}{B(Z \rightarrow \mu\mu)} \frac{\varepsilon_{\#_T}^{\text{Trigger}}}{\varepsilon_{\mu\tau}^{\text{Trigger}}} \varepsilon_{\mu\tau}^{\#_T}. \quad (7)$$

Since there is no prompt production of a genuine τ_h in the $Z(\rightarrow \mu\mu) + \text{jets}$ sample, $\alpha_{\tau j} = 0$ and $\alpha_{\tau\tau} = 0$. The $Z(\rightarrow \nu\nu) + \text{jets}$ contribution to the SR is calculated as:

$$N_{Z \rightarrow \nu\nu + \text{jets}}^{\text{SR}} = \frac{N_{Z \rightarrow \mu\mu + \text{jets}}^{\text{CR}}}{A_\mu^2\varepsilon_\mu^{\text{reco}2}} R \frac{\varepsilon_{\#_T}^{\text{Trigger}}}{\varepsilon_{\mu\tau}^{\text{Trigger}}} \varepsilon_{\mu\tau}^{\#_T} \mathcal{P}(2), \quad (8)$$

where $\varepsilon_{\#_T}^{\text{Trigger}}$ is the $\#_T$ trigger efficiency and $\varepsilon_{\mu\tau}^{\text{Trigger}}$ the $\mu\tau_h$ trigger efficiency. The efficiency for the $\#_T > 250 \text{ GeV}$ signal selection ($\varepsilon^{\#_T}$) is determined by calculating the fraction of the observed events in the CR that have $\#_T > 250 \text{ GeV}$. The muon identification efficiency ε_μ is measured using a “tag-and-probe” method. The probability for a jet to be misidentified as a τ_h lepton has a measured value of $f = 0.016 \pm 0.002$. The estimated $Z(\rightarrow \nu\nu) + \text{jets}$ contribution to the SR is determined to be $N_{Z \rightarrow \nu\nu}^{\text{SR}} = 0.03 \pm 0.02$.

6.2.3 Estimate of the $Z(\rightarrow \tau\tau) + \text{jets}$ event background to the multiple- τ_h final state

The contribution from $Z \rightarrow \tau\tau$ events is determined with the $Z(\rightarrow \mu\mu) + \text{jets}$ CR sample used to estimate the background from $Z(\rightarrow \nu\nu) + \text{jets}$, with the muons treated as τ_h leptons. The α_{xy} factors are more difficult to estimate for $Z \rightarrow \tau\tau$ events since there are several ways in which $Z \rightarrow \tau\tau$ events can contribute to the SR: (i) both τ_h leptons pass the kinematic acceptance and identification criteria; (ii) both τ_h leptons pass the kinematic acceptance criteria, but only one passes the identification criteria; (iii) one τ_h fails the kinematic acceptance criteria, while the other τ_h passes both the kinematic acceptance and identification criteria; or (iv) both τ_h leptons fail the kinematic acceptance criteria. The $Z(\rightarrow \tau\tau) + \text{jets}$ contribution to the SR is calculated as:

$$N_{Z \rightarrow \tau\tau}^{\text{SR}} = N_{Z \rightarrow \mu\mu}^{\text{CR}} R \left[\frac{A_\tau^2\varepsilon_\tau^2}{A_\mu^2\varepsilon_\mu^{\text{reco}2}} + \frac{2A_\tau^2\varepsilon_\tau(1-\varepsilon_\tau)}{A_\mu^2\varepsilon_\mu^{\text{reco}2}} \mathcal{P}(1) + \frac{2A_\tau(1-A_\tau)\varepsilon_\tau}{A_\mu^2\varepsilon_\mu^{\text{reco}2}} \mathcal{P}(1) + \frac{(1-A_\tau)^2}{A_\mu^2\varepsilon_\mu^{\text{reco}2}} \mathcal{P}(2) \right], \quad (9)$$

where R is given by:

$$\frac{B(Z \rightarrow \tau\tau)B^2(\tau \rightarrow \tau_h)}{B(Z \rightarrow \mu\mu)} \frac{\varepsilon_{\#_T}^{\text{Trig}}}{\varepsilon_{\mu\tau}^{\text{Trig}}} \varepsilon_{\mu\tau}^{\#_T}, \quad (10)$$

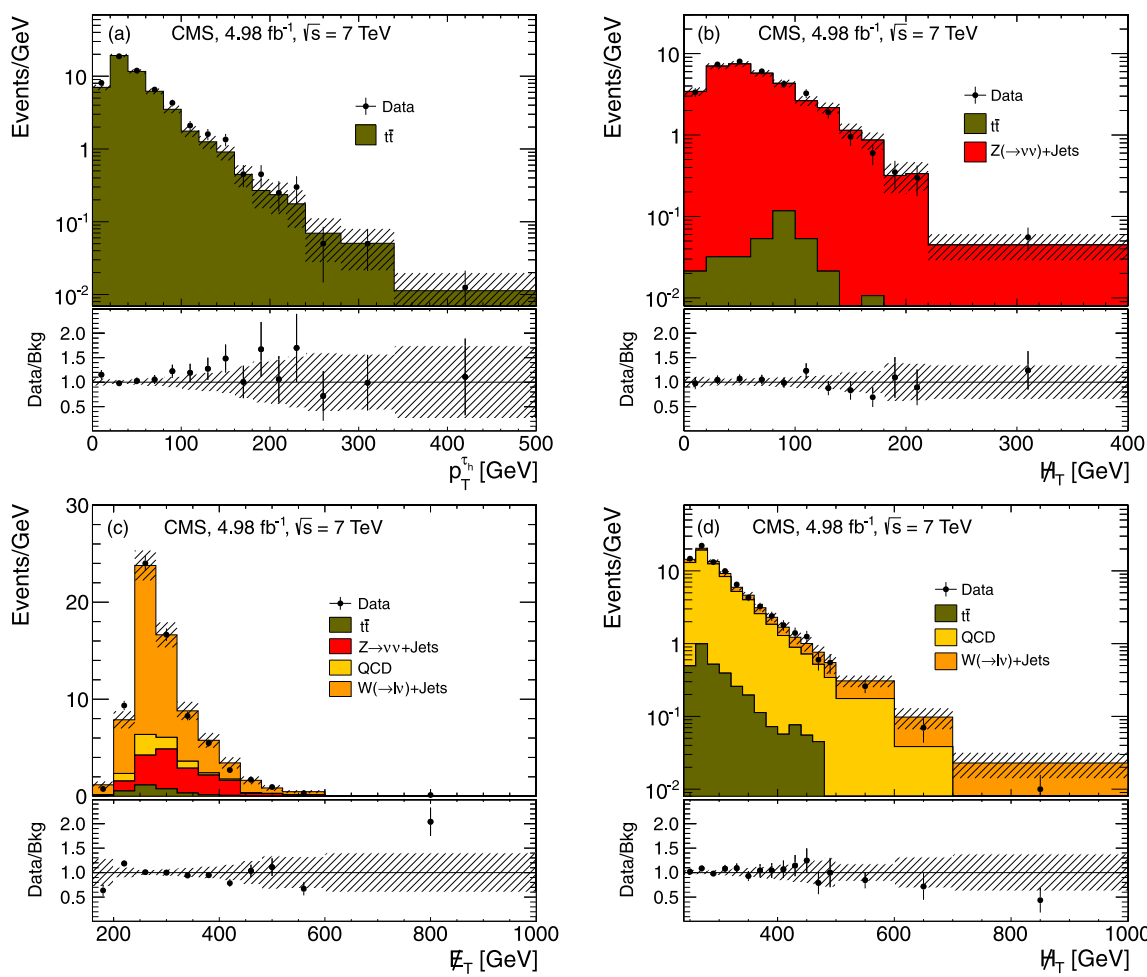


Fig. 4 Data-to-MC comparison for the multiple- τ_h final state: **(a)** the p_T distribution of the τ_h candidate in the $t\bar{t}$ CR; **(b)** η_T distribution in the $Z(\rightarrow \nu\nu) + \text{jets}$ CR; **(c)** η_T distribution in the $W + \text{jets}$ CR; and **(d)** η_T distribution with the requirement $|\Delta\phi(j_2, \eta_T)| < 0.1$. The bottom panes show the ratio between data and background while the hatched area depicts the total uncertainty on the MC

A_{τ} is the τ_h acceptance, ε_{τ} is the τ_h identification efficiency in this control sample, and $f = 0.016 \pm 0.002$. The estimated $Z(\rightarrow \tau\tau) + \text{jets}$ contribution to the SR is determined to be $N_{Z(\rightarrow \tau\tau)}^{\text{SR}} = 0.21 \pm 0.13$.

6.2.4 Estimate of the $W + \text{jets}$ event background to the multiple- τ_h final state

To select the $W + \text{jets}$ CR, the τ_h isolation requirement, which discriminates between a τ_h lepton and other jets, is removed from the SR selection requirements. However, the lack of the τ_h isolation requirement increases the contribution from other backgrounds as most of the backgrounds arise because jets are misidentified as a τ_h lepton. To minimize the contribution from $t\bar{t}$ production, events are required to have no jets identified as a b jet. This requirement reduces the contamination from $t\bar{t}$ events to around 5 %. The purity

of the $W + \text{jets}$ CR is approximately 65 %. Figure 4(c) shows the η_T distribution, defined as the magnitude of the negative of the vector sum of the transverse momentum of all PF objects in the event, for events in the $W + \text{jets}$ CR. The contributions of QCD multijet, $t\bar{t}$, and $Z(\rightarrow \nu\nu) + \text{jets}$ events are subtracted in order to determine the number of $W + \text{jets}$ events in the CR. The predicted rates for QCD multijet, $t\bar{t}$, and $Z(\rightarrow \nu\nu) + \text{jets}$ events are determined by extrapolating from their corresponding CRs. Since there is no genuine multiple- τ_h production in $W + \text{jets}$, $\alpha_{\tau\tau} = 0$. According to simulation, the fraction of events in the CR with one genuine τ_h is $A_{\tau j} = 0.149 \pm 0.016$, while the fraction of events without a genuine τ_h is $A_{jj} = 0.851 \pm 0.038$. Therefore, $\alpha_{\tau j}$ in Eq. (4) is given by $A_{\tau j}\varepsilon_{\tau}^{\text{iso}}/P(0 \text{ b jets})$, where $\varepsilon_{\tau}^{\text{iso}}$ is the probability for a τ_h to pass the isolation requirement and $P(0 \text{ b jets})$ is the probability to not have any light-quark or gluon jet misidentified as a b jet. Similarly, α_{jj} is given by $A_{jj}/P(0 \text{ b jets})$. The contribution of $W + \text{jets}$ events to the

SR is then calculated as:

$$N_{W+\text{jets}}^{\text{SR}} = \frac{N_{W+\text{jets}}^{\text{After subtraction}}}{P(0 \text{ b jets})} [A_{\tau j} \varepsilon_{\tau}^{\text{iso}} \mathcal{P}(1) + A_{jj} \mathcal{P}(2)]. \quad (11)$$

The average rate at which jets are misidentified as a τ_h lepton is measured to be 0.019 ± 0.001 . The rate f_b at which light-quark jets or gluon jets are misidentified as a b jet is used to determine $P(0 \text{ b jets})$. The estimated $W + \text{jets}$ contribution to the SR is determined to be $N_{W+\text{jets}}^{\text{SR}} = 5.20 \pm 0.63$.

6.2.5 Estimate of the QCD multijet event background to the multiple- τ_h final state

QCD multijet events contribute to the multiple- τ_h SR when mismeasurements of jet energies lead to large values of \cancel{H}_T and when jets are misidentified as τ_h candidates. By removing the τ_h isolation criteria and inverting the $|\Delta\phi(j_2, \cancel{H}_T)|$ requirement, a QCD CR sample with about 99 % purity is obtained. Figure 4(d) shows the expected and observed \cancel{H}_T distributions for this sample. A scale factor is obtained from this CR and used to correct the signal prediction for QCD multijet events in simulation. The estimated contribution to the SR from QCD multijet events is determined to be $N_{\text{QCD}}^{\text{SR}} = 0.02 \pm 0.02$.

7 Systematic uncertainties

Systematic uncertainties are taken into account for both signal and background events and are described separately. Both the signal and background are affected by the systematic uncertainty in the identification of the τ_h candidate. The systematic uncertainty for τ_h identification is obtained using a $Z \rightarrow \tau\tau$ enhanced region and by correcting this cross section by that measured for $Z \rightarrow ee$ and $Z \rightarrow \mu\mu$ events. This uncertainty is validated on a control sample of $Z \rightarrow \tau\tau$ events. The level of agreement between data and simulation is found to be at the level of 7 %. Further validation of the performance of τ_h identification in a SUSY-like environment is performed by selecting a $W(\rightarrow \tau\nu \rightarrow \tau_h\nu\nu) + \text{jets}$ CR with large hadronic activity (H_T) and large transverse momentum imbalance (\cancel{H}_T). The level of agreement between the predicted rate for $W(\rightarrow \tau\nu \rightarrow \tau_h\nu\nu)$ events and the observed number of events is within 7 % and is determined as a function of H_T and \cancel{H}_T .

7.1 Systematic uncertainties on background events

The principal sources of systematic uncertainty on the background predictions arise from the correction factors, the finite number of events in the CRs, the measured rates at which jets are misidentified as a τ_h lepton, and the level of

agreement between the observed and predicted numbers of events in CRs.

The contributions to the uncertainties on the correction factors are different for each background category. The dominant effect is due to the uncertainty in the τ_h identification efficiency. In the multiple- τ_h final state, uncertainties in the jet-energy scale (JES) [33] and the τ_h -energy scale (TES) [34] are used to evaluate how changes in H_T , \cancel{H}_T , and jet kinematics affect the correction factors. The systematic uncertainty on the correction factors due to the JES and TES is at most ~ 3 % for all backgrounds. Smaller contributions to the uncertainties in the correction factors arise from the muon reconstruction and isolation efficiency (<1 %), the uncertainty in the branching fractions ($\ll 1$ %), and the uncertainties in trigger efficiency (1 %).

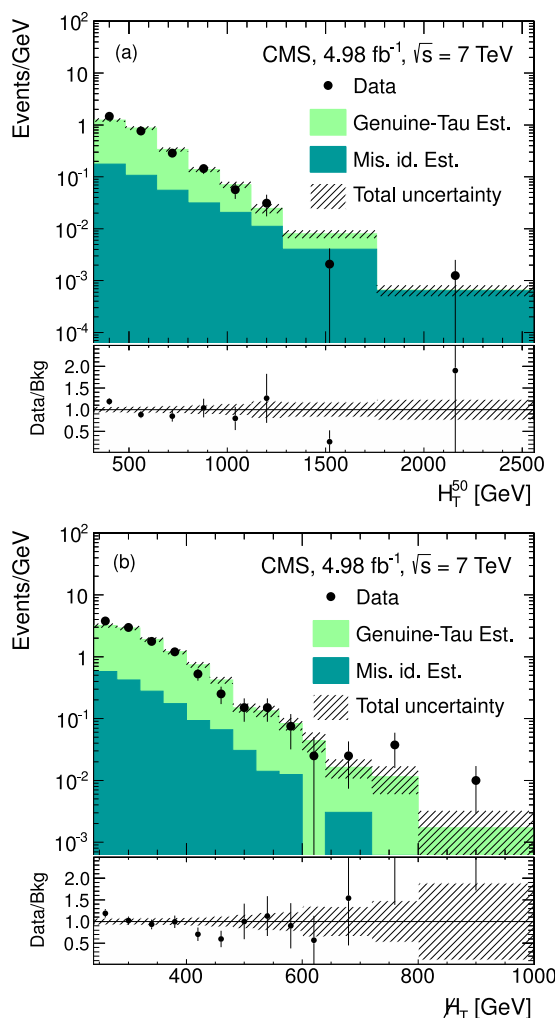
The systematic uncertainties on the measured rates for jet misidentification as a τ_h lepton are dominated by the size of the jet sample used to measure these rates and range from 2 % for the single- τ_h final state to 5.6–10 % for the multiple- τ_h final state. The level of agreement between the observed and predicted number of events in MC studies of the CRs is used to assign an additional systematic uncertainty and ranges from 2 % for the single- τ_h final state to 3 % for the multiple- τ_h final state. Finally, the systematic uncertainty arising from statistical uncertainties on the number of events in the CRs ranges from 2–5 % for the multiple- τ_h final state to 3–10 % for the single- τ_h final state.

7.2 Systematic uncertainties on signal events

The main sources of systematic uncertainties in the SR are due to trigger efficiencies, identification efficiencies, the energy, and momentum scales, the luminosity measurement and PDFs. The uncertainty on the luminosity measurement is 2.2 % [35]. Systematic uncertainties on the \cancel{H}_T triggers (2.5 %) are measured using a sample in which around 99 % of the events are $t\bar{t}$ events, which have a similar topology to events in the SR samples. The systematic uncertainties on the TES and JES (3.0 %) yield an uncertainty on the signal acceptance of 2.3 %. The uncertainty on the \cancel{H}_T scale depends on the uncertainty of the JES (2–5 % depending on the η and p_T values of the jet) and on the unclustered energy scale (10 %). Unclustered energy is defined as the energy found “outside” any reconstructed lepton or jet with $p_T > 10$ GeV. The unclustered energy scale uncertainty has a negligible systematic uncertainty on the signal acceptance. The systematic uncertainty due to imprecise knowledge of the PDFs (11 %) is determined by comparing the CTEQ6.6L [36], MSTW 2008 NLO [37], and NNPDF2.1 [38] PDFs with the default PDF [39]. The systematic uncertainty due to the imprecise modeling of the initial-state and final-state radiation [40] is negligible ($\ll 1$ %). The systematic uncertainties associated with event pileup are also

Table 3 Number of data and estimated background events with statistical and systematic uncertainties, respectively, in the single- τ_h final state

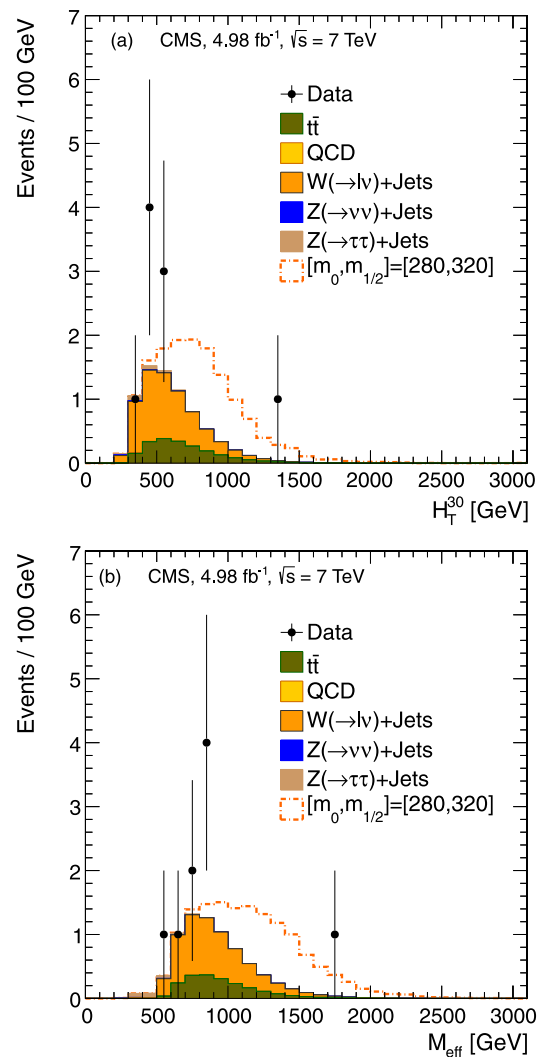
Process	Baseline	Signal region
Fake- τ_h	$67 \pm 2 \pm 19$	$3.4 \pm 0.4 \pm 1.0$
Real- τ_h	$367 \pm 10 \pm 27$	$25.9 \pm 2.5 \pm 2.3$
Estimated $\sum SM$	$434 \pm 10 \pm 33$	$29.3 \pm 2.6 \pm 2.5$
Data	444	28

**Fig. 5** Distributions of (a) H_T^{50} , and (b) μ_T for the single- τ_h final state. The points with errors represent data that satisfy the baseline selection while the filled green (light) and filled blue (dark) areas shows the predicted backgrounds due to events containing a genuine τ_h and a misidentified τ_h , respectively. The hatched area shows the total uncertainty on the prediction (Color figure online)

negligible. Uncertainties on the theoretical cross sections are evaluated by varying the PDFs and by changing the renormalization and factorization scales by a factor of two [26–31].

Table 4 Number of data and estimated background events with statistical and systematic uncertainties, respectively, in the multiple- τ_h final state

Process	Signal region
QCD multijet events	$0.02 \pm 0.02 \pm 0.17$
W + jets	$5.20 \pm 0.63 \pm 0.62$
t̄t	$2.03 \pm 0.36 \pm 0.34$
Z($\rightarrow \tau\tau$) + jets	$0.21 \pm 0.13 \pm 0.17$
Z($\rightarrow vv$) + jets	$0.03 \pm 0.02 \pm 0.50$
Estimated $\sum SM$	$7.49 \pm 0.74 \pm 0.90$
Data	9

**Fig. 6** Stacked distributions of (a) H_T^{30} , and (b) M_{eff} in the SR for the multiple- τ_h final state. The background distributions are taken from MC events that are normalized to the predictions based on data over the full region. The shapes obtained from MC simulation are used for illustrative purposes only

8 Results

For the single- τ_h final state, the number of background events containing a genuine τ_h , as well as the number of background events containing a misidentified τ_h , are estimated with data. The results for the baseline and the full selection are listed in Table 3. Figure 5 shows the H_T^{50} and \cancel{H}_T distributions of data and the different background predictions. The observed number of events in data is in agreement with the SM predictions.

The largest sources of background for the multiple- τ_h final state are from $t\bar{t}$ and $W + \text{jets}$ events. A counting experiment is performed and the background predictions from data are compared with the observed number of events. Table 4 lists these background predictions and the observed number of events in the SR. Figure 6 shows the H_T^{30} as well as the M_{eff} distributions in the SR, where M_{eff} is the sum $\cancel{H}_T + H_T^{30}$. The background distributions in Fig. 6 are taken from simulation and normalized over the full spectrum. The estimated number of events due to the SM background processes is in agreement with the number of observed events in the SR.

9 Limits on new physics

The observed numbers of events in the single- τ_h and multiple- τ_h final states do not reveal any evidence of physics beyond the standard model. Exclusion limits are set using the CL_s [41] criterion in the context of the CMSSM [42]. The CMSSM parameter space with $\tan\beta = 40$, $A_0 = -500$ GeV, $\mu > 0$, and $M_t = 173.2$ GeV is chosen as a possible scenario with a light $\tilde{\tau}$ and a value of $\Delta M \leq 20$ GeV. The excluded regions are shown for the single- τ_h and multiple- τ_h final states in Figs. 7(a) and 7(b), respectively. The limits are set using a simple counting experiment. Systematic uncertainties are treated as nuisance parameters and marginalized, and contamination from signal events in the control samples is taken into account. In the CL_s method, both the background-only as well as the signal + background hypothesis are used to derive the confidence levels CL_s and the resulting limits and the uncertainty bands on the exclusion contours. In the case of very small values of ΔM (~ 5 GeV), the lower-energy τ_h cannot be effectively detected and only the energetic τ_h from the decay of the neutralino can be observed. The search for new physics with a single τ lepton has a better sensitivity in this case. The single- τ_h and multiple- τ_h topologies thus have complementary sensitivity and together provide coverage for models with a wide range of ΔM values.

Using the limits set by the single- τ_h analysis, a common gaugino mass $m_{1/2}$ of <495 GeV is excluded at 95 % Confidence Level (CL) for a common scalar mass m_0 of

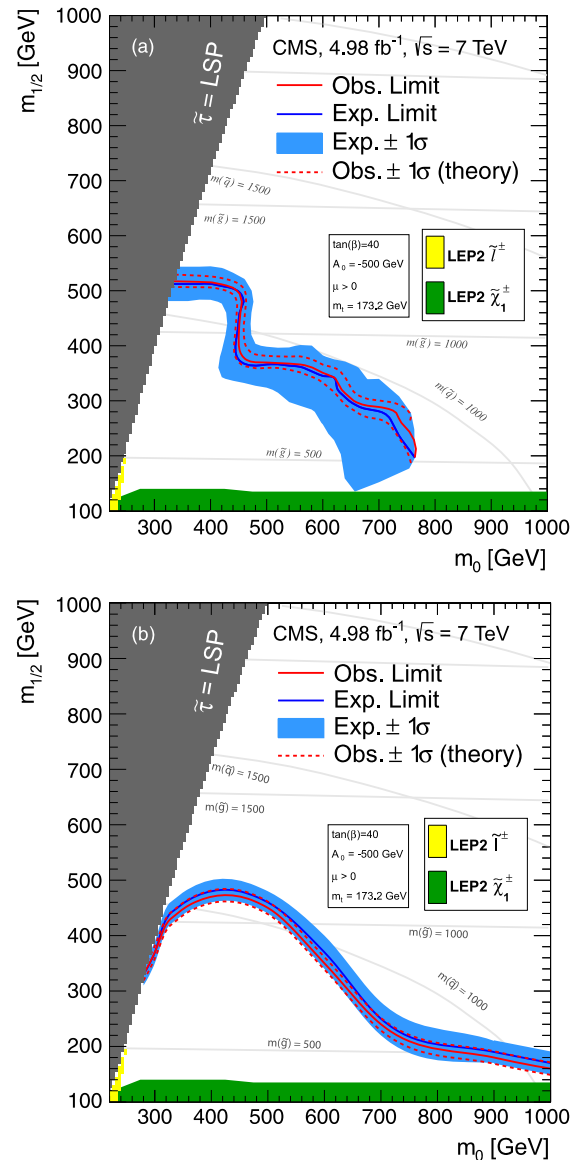


Fig. 7 95 % CL exclusion limits in the CMSSM plane at $\tan\beta = 40$ for: (a) Single- τ_h final state, and (b) multiple- τ_h final state. In the figures shown, the solid red line (Obs. Limit) denotes the experimental limit while the dotted red lines (Obs. $\pm\sigma$ (theory)) represent the uncertainty on the experimental limit due to uncertainties on the theoretical cross sections. The blue band (Exp. $\pm\sigma$) represents the expected uncertainties. The contours of constant squark and gluino mass are in units of GeV (Color figure online)

<440 GeV. For the multiple- τ_h analysis, $m_{1/2} < 465$ GeV is excluded at 95 % CL for $m_0 = 440$ GeV. A gluino with mass <1.15 TeV is excluded at 95 % CL for $m_0 < 440$ GeV. It can be noted that the single- τ_h analysis shows better sensitivity for small values of ΔM , which is near the boundary of $\tilde{\tau} = \text{LSP}$.

The results for the multiple- τ_h final states are also interpreted in the context of SMS [13]. The $\tau\tau$ SMS scenario (T3tauh) is studied where gluinos are produced in pairs and subsequently decay to τ lepton pairs and an LSP via a neu-

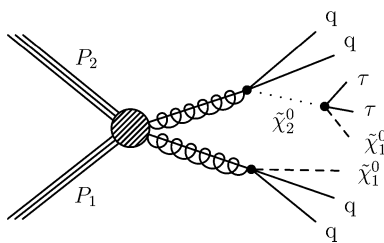


Fig. 8 Diagram for the T3tauh SMS model

tralino ($\tilde{g} \rightarrow q\bar{q}\tilde{\chi}_2^0$, $\tilde{\chi}_2^0 \rightarrow \tau\bar{\tau} \rightarrow \tau\tau\tilde{\chi}_1^0$). The diagram for the T3tauh model is given in Fig. 8. A gluino mass of <740 GeV is excluded at 95 % CL for LSP masses up to 205 GeV (here, the mass of $\tilde{\chi}_2^0$ is the average of the masses of the gluino and the LSP). Figure 9(a) shows the 95 % CL exclusion region obtained for T3tauh. The limits on the mass of the gluino and LSP are shown with a solid red line.

In the simplified GMSB scenario, the $\tilde{\tau}$ is the NLSP and decays to a τ lepton and a gravitino \tilde{G} , with a mass of the order of \sim keV [43–45] ($\tilde{\chi}_2^0 \rightarrow \tau\tilde{\tau} \rightarrow \tau\tau\tilde{G}$). The topology for this simplified GMSB scenario is similar to that of T3tauh except for the assumption that both the gluinos decay to τ -lepton pairs with a branching fraction of 100 %. Therefore, the results are also interpreted in the simplified GMSB scenario using the T3tauh scenario. The signal acceptance is corrected to account for the final state containing up to four τ leptons. A gluino with mass <860 GeV is excluded at 95 % CL. Figure 9(b) shows the exclusion limits for the simplified GMSB scenario as a function of the gluino mass.

Since the SMS topologies considered in this paper are characterized by two τ leptons in the final state, we do not present SMS limits for the single- τ_h final state.

10 Summary

A search for physics beyond the standard model with one or more hadronically decaying τ leptons, highly energetic jets, and large transverse momentum imbalance in the final state is presented. The data sample corresponds to an integrated luminosity of 4.98 ± 0.11 fb^{-1} of pp collisions at $\sqrt{s} = 7$ TeV collected with the CMS detector. The final number of events selected in data is consistent with the predictions for standard model processes. We set upper limits on the cross sections for the CMSSM, GMSB, and SMS scenarios. Within the CMSSM framework at $\tan\beta = 40$, a gaugino mass $m_{1/2} < 495$ GeV is excluded at 95 % CL for scalar masses $m_0 < 440$ GeV. This result sets a lower limit on the mass of the gluino at 1.15 TeV with 95 % CL in this region. In the multiple- τ_h final state, a gluino with a mass less than 740 GeV is excluded for the T3tauh simplified model while a gluino with a mass less than 860 GeV is excluded for the simplified GMSB scenario at 95 % CL.

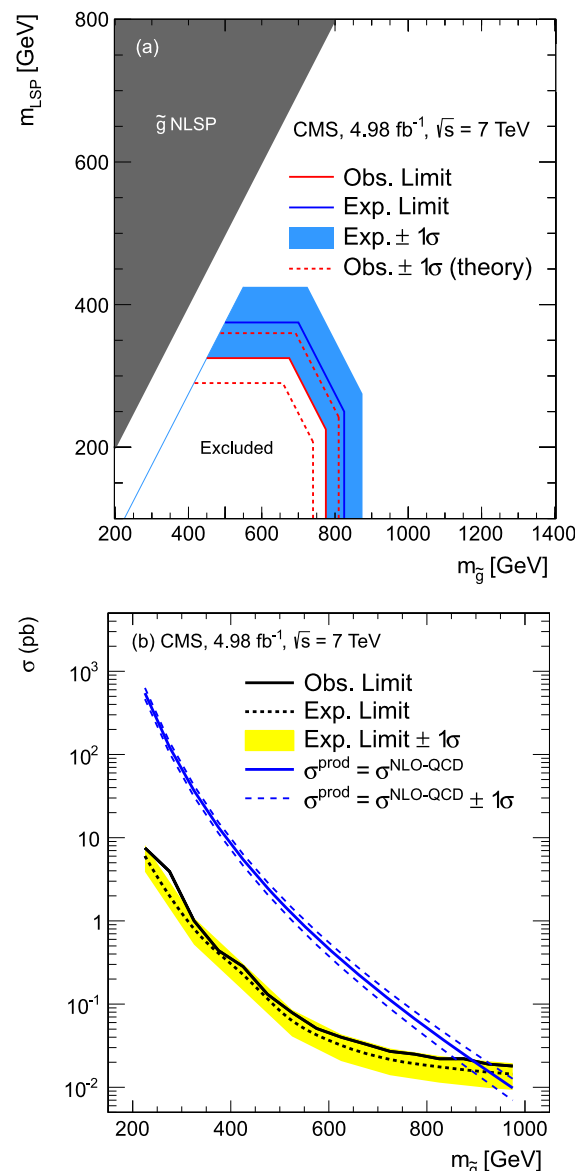


Fig. 9 Exclusion limits for the multiple- τ_h final state: (a) 95 % CL exclusion region obtained for the T3tauh model, where the solid red line represents the limits on the mass of the gluino and the LSP; (b) 95 % CL cross section upper limits as a function of gluino mass in the GMSB scenario. In this figure σ^{prod} represents the cross section for the production of a pair of gluinos with subsequent decay into τ lepton pairs at a 100 % branching fraction (Color figure online)

Acknowledgements We congratulate our colleagues in the CERN accelerator departments for the excellent performance of the LHC and thank the technical and administrative staffs at CERN and at other CMS institutes for their contributions to the success of the CMS effort. In addition, we gratefully acknowledge the computing centres and personnel of the Worldwide LHC Computing Grid for delivering so effectively the computing infrastructure essential to our analyses. Finally, we acknowledge the enduring support for the construction and operation of the LHC and the CMS detector provided by the following funding agencies: the Austrian Federal Ministry of Science and Research; the Belgian Fonds de la Recherche Scientifique, and Fonds voor Wetenschappelijk Onderzoek; the Brazilian Funding Agencies

(CNPq, CAPES, FAPERJ, and FAPESP); the Bulgarian Ministry of Education and Science; CERN; the Chinese Academy of Sciences, Ministry of Science and Technology, and National Natural Science Foundation of China; the Colombian Funding Agency (COLCIENCIAS); the Croatian Ministry of Science, Education and Sport; the Research Promotion Foundation, Cyprus; the Ministry of Education and Research, Recurrent financing contract SF0690030s09 and European Regional Development Fund, Estonia; the Academy of Finland, Finnish Ministry of Education and Culture, and Helsinki Institute of Physics; the Institut National de Physique Nucléaire et de Physique des Particules/CNRS, and Commissariat à l'Énergie Atomique et aux Énergies Alternatives/CEA, France; the Bundesministerium für Bildung und Forschung, Deutsche Forschungsgemeinschaft, and Helmholtz-Gemeinschaft Deutscher Forschungszentren, Germany; the General Secretariat for Research and Technology, Greece; the National Scientific Research Foundation, and National Office for Research and Technology, Hungary; the Department of Atomic Energy and the Department of Science and Technology, India; the Institute for Studies in Theoretical Physics and Mathematics, Iran; the Science Foundation, Ireland; the Istituto Nazionale di Fisica Nucleare, Italy; the Korean Ministry of Education, Science and Technology and the World Class University program of NRF, Korea; the Lithuanian Academy of Sciences; the Mexican Funding Agencies (CINVESTAV, CONACYT, SEP, and UASLP-FAI); the Ministry of Science and Innovation, New Zealand; the Pakistan Atomic Energy Commission; the Ministry of Science and Higher Education and the National Science Centre, Poland; the Fundação para a Ciência e a Tecnologia, Portugal; JINR (Armenia, Belarus, Georgia, Ukraine, Uzbekistan); the Ministry of Education and Science of the Russian Federation, the Federal Agency of Atomic Energy of the Russian Federation, Russian Academy of Sciences, and the Russian Foundation for Basic Research; the Ministry of Science and Technological Development of Serbia; the Secretaría de Estado de Investigación, Desarrollo e Innovación and Programa Consolider-Ingenio 2010, Spain; the Swiss Funding Agencies (ETH Board, ETH Zurich, PSI, SNF, UniZH, Canton Zurich, and SER); the National Science Council, Taipei; the Scientific and Technical Research Council of Turkey, and Turkish Atomic Energy Authority; the Science and Technology Facilities Council, UK; the US Department of Energy, and the US National Science Foundation.

Individuals have received support from the Marie-Curie programme and the European Research Council (European Union); the Leventis Foundation; the A.P. Sloan Foundation; the Alexander von Humboldt Foundation; the Austrian Science Fund (FWF); the Belgian Federal Science Policy Office; the Fonds pour la Formation à la Recherche dans l'Industrie et dans l'Agriculture (FRIA-Belgium); the Agentschap voor Innovatie door Wetenschap en Technologie (IWT-Belgium); the Council of Science and Industrial Research, India; the Compagnia di San Paolo (Torino); the HOMING PLUS programme of Foundation for Polish Science, cofinanced from European Union, Regional Development Fund; and the Norman Hackerman Advanced Research Program.

Open Access This article is distributed under the terms of the Creative Commons Attribution License which permits any use, distribution, and reproduction in any medium, provided the original author(s) and the source are credited.

References

- J.F. Gunion et al., *The Higgs Hunter's Guide* (2000), Westview Press
- E. Komatsu et al., Seven-year Wilkinson microwave anisotropy probe (WMAP) observations: cosmological interpretation. *Astrophys. J. Suppl.* **192**, 18 (2011). doi:[10.1088/0067-0049/192/2/18](https://doi.org/10.1088/0067-0049/192/2/18), arXiv:[1001.4538](https://arxiv.org/abs/1001.4538)
- S.P. Martin, A supersymmetry primer (1997). arXiv:[hep-ph/9709356](https://arxiv.org/abs/hep-ph/9709356)
- J. Wess, B. Zumino, Supergauge transformations in four-dimensions. *Nucl. Phys. B* **70**, 39 (1974). doi:[10.1016/0550-3213\(74\)90355-1](https://doi.org/10.1016/0550-3213(74)90355-1)
- A.H. Chamseddine, R. Arnowitt, P. Nath, Locally supersymmetric grand unification. *Phys. Rev. Lett.* **49**, 970 (1982). doi:[10.1103/PhysRevLett.49.970](https://doi.org/10.1103/PhysRevLett.49.970)
- L. Hall, J. Lykken, S. Weinberg, Supergravity as the messenger of supersymmetry breaking. *Phys. Rev. D* **27**, 2359 (1983). doi:[10.1103/PhysRevD.27.2359](https://doi.org/10.1103/PhysRevD.27.2359)
- K. Griest, D. Seckel, Three exceptions in the calculation of relic abundances. *Phys. Rev. D* **43**, 3191 (1991). doi:[10.1103/PhysRevD.43.3191](https://doi.org/10.1103/PhysRevD.43.3191)
- R. Arnowitt et al., Determining the dark matter relic density in the minimal supergravity stau-neutralino coannihilation region at the large hadron collider. *Phys. Rev. Lett.* **100**, 231802 (2008). doi:[10.1103/PhysRevLett.100.231802](https://doi.org/10.1103/PhysRevLett.100.231802), arXiv:[0802.2968](https://arxiv.org/abs/0802.2968)
- CMS Collaboration, The CMS experiment at the CERN LHC. *J. Instrum.* **03**, S08004 (2008). doi:[10.1088/1748-0221/3/08/S08004](https://doi.org/10.1088/1748-0221/3/08/S08004)
- G.L. Kane et al., Study of constrained minimal supersymmetry. *Phys. Rev. D* **49**, 6173 (1994). doi:[10.1103/PhysRevD.49.6173](https://doi.org/10.1103/PhysRevD.49.6173), arXiv:[hep-ph/9312272](https://arxiv.org/abs/hep-ph/9312272)
- A.H. Chamseddine, R.L. Arnowitt, P. Nath, Locally supersymmetric grand unification. *Phys. Rev. Lett.* **49**, 970 (1982). doi:[10.1103/PhysRevLett.49.970](https://doi.org/10.1103/PhysRevLett.49.970)
- J. Alwall, P.C. Schuster, N. Toro, Simplified models for a first characterization of new physics at the LHC. *Phys. Rev. D* **79**, 075020 (2009). doi:[10.1103/PhysRevD.79.075020](https://doi.org/10.1103/PhysRevD.79.075020), arXiv:[0810.3921](https://arxiv.org/abs/0810.3921)
- D. Alves et al., Simplified models for LHC new physics searches. *J. Phys. G* **39**, 105005 (2012). doi:[10.1088/0954-3899/39/10/105005](https://doi.org/10.1088/0954-3899/39/10/105005), arXiv:[1105.2838](https://arxiv.org/abs/1105.2838)
- ATLAS Collaboration, Search for supersymmetry in events with large missing transverse momentum, jets, and at least one tau lepton in 7 TeV proton–proton collision data with the ATLAS detector. *Eur. Phys. J. C* **72**, 2215 (2012). doi:[10.1140/epjc/s10052-012-2215-7](https://doi.org/10.1140/epjc/s10052-012-2215-7), arXiv:[1210.1314](https://arxiv.org/abs/1210.1314)
- CMS Collaboration, Commissioning of the particle-flow reconstruction in minimum-bias and jet events from pp collisions at 7 TeV. CMS Physics Analysis Summary CMS-PAS-PFT-10-002 (2010)
- M. Cacciari, G.P. Salam, G. Soyez, The anti- k_t jet clustering algorithm. *J. High Energy Phys.* **04**, 063 (2008). doi:[10.1088/1126-6708/2008/04/063](https://doi.org/10.1088/1126-6708/2008/04/063), arXiv:[0802.1189](https://arxiv.org/abs/0802.1189)
- CMS Collaboration, Performance of muon identification in pp collisions at $\sqrt{s} = 7$ TeV. CMS Physics Analysis Summary CMS-PAS-MUO-10-002 (2010)
- CMS Collaboration, Electron reconstruction and identification at $\sqrt{s} = 7$ TeV. CMS physics analysis summary CMS-PAS-EGM-10-004 (2010)
- CMS Collaboration, Performance of tau reconstruction algorithms in 2010 data collected with CMS. CMS Physics Analysis Summary CMS-PAS-TAU-11-001 (2011)
- T. Sjöstrand, S. Mrenna, P.Z. Skands, PYTHIA 6.4 physics and manual. *J. High Energy Phys.* **05**, 026 (2006). doi:[10.1088/1126-6708/2006/05/026](https://doi.org/10.1088/1126-6708/2006/05/026), arXiv:[hep-ph/0603175](https://arxiv.org/abs/hep-ph/0603175)
- J. Alwall, MadGraph/MadEvent v4: the new web generation. *J. High Energy Phys.* **09**, 028 (2008). doi:[10.1088/1126-6708/2007/09/028](https://doi.org/10.1088/1126-6708/2007/09/028), arXiv:[0706.2334](https://arxiv.org/abs/0706.2334)
- CMS Collaboration, Measurement of the underlying event activity at the LHC with $\sqrt{s} = 7$ TeV and comparison with $\sqrt{s} = 0.9$ TeV. *J. High Energy Phys.* **09**, 109 (2011). doi:[10.1007/JHEP09\(2011\)109](https://doi.org/10.1007/JHEP09(2011)109), arXiv:[1107.0330](https://arxiv.org/abs/1107.0330)
- J. Pumplin et al., New generation of parton distributions with uncertainties from global QCD analysis. *J. High Energy Phys.* **07**,

- 012 (2002). doi:[10.1088/1126-6708/2002/07/012](https://doi.org/10.1088/1126-6708/2002/07/012), arXiv:hep-ph/0201195
24. Z. Wąs, TAUOLA the library for tau lepton decay. Nucl. Phys. B, Proc. Suppl. **98**, 96 (2001). doi:[10.1016/S0920-5632\(01\)01200-2](https://doi.org/10.1016/S0920-5632(01)01200-2), arXiv:hep-ph/0011305
25. GEANT4 Collaboration, GEANT4—a simulation toolkit. Nucl. Instrum. Methods **506**, 250 (2003). doi:[10.1016/S0168-9002\(03\)01368-8](https://doi.org/10.1016/S0168-9002(03)01368-8)
26. M. Krämer et al., Supersymmetry production cross sections in pp collisions at $\sqrt{s} = 7$ TeV (2012). arXiv:1206.2892
27. W. Beenakker et al., Squark and gluino production at hadron colliders. Nucl. Phys. B **492**, 51 (1997). doi:[10.1016/S0550-3213\(97\)80027-2](https://doi.org/10.1016/S0550-3213(97)80027-2)
28. A. Kulesza, L. Motyka, Threshold resummation for squark–antisquark and gluino-pair production at the LHC. Phys. Rev. Lett. **102**, 111802 (2009). doi:[10.1103/PhysRevLett.102.111802](https://doi.org/10.1103/PhysRevLett.102.111802)
29. A. Kulesza, L. Motyka, Soft gluon resummation for the production of gluino–gluino and squark–antisquark pairs at the LHC. Phys. Rev. D **80**, 095004 (2009). doi:[10.1103/PhysRevD.80.095004](https://doi.org/10.1103/PhysRevD.80.095004), arXiv:0905.4749
30. W. Beenakker et al., Soft-gluon resummation for squark and gluino hadroproduction. J. High Energy Phys. **0912**, 041 (2009). doi:[10.1088/1126-6708/2009/12/041](https://doi.org/10.1088/1126-6708/2009/12/041), arXiv:0909.4418
31. W. Beenakker et al., Squark and gluino hadroproduction. Int. J. Mod. Phys. A **26**, 2637 (2011). doi:[10.1142/S0217751X11053560](https://doi.org/10.1142/S0217751X11053560)
32. CMS Collaboration, b-jet identification in the CMS experiment. CMS physics analysis summary CMS-PAS-BTV-11-004 (2011)
33. CMS Collaboration, Determination of jet energy calibration and transverse momentum resolution in CMS. J. Instrum. **06**, P11002 (2011). doi:[10.1088/1748-0221/6/11/P11002](https://doi.org/10.1088/1748-0221/6/11/P11002), arXiv:1107.4277
34. CMS Collaboration, Performance of τ -lepton reconstruction and identification in CMS. J. Instrum. **7**, P01001 (2011). doi:[10.1088/1748-0221/7/01/P01001](https://doi.org/10.1088/1748-0221/7/01/P01001)
35. CMS Collaboration, Absolute calibration of the luminosity measurement at CMS: winter 2012 update. CMS physics analysis summary CMS-PAS-SMP-12-008 (2012)
36. P.M. Nadolsky et al., Implications of CTEQ global analysis for collider observables. Phys. Rev. D **78**, 013004 (2008). doi:[10.1103/PhysRevD.78.013004](https://doi.org/10.1103/PhysRevD.78.013004), arXiv:0802.0007
37. A.D. Martin et al., Parton distributions for the LHC. Eur. Phys. J. C **63**, 189 (2009). doi:[10.1140/epjc/s10052-009-1072-5](https://doi.org/10.1140/epjc/s10052-009-1072-5), arXiv:0901.0002
38. R.D. Ball et al., A first unbiased global NLO determination of parton distributions and their uncertainties. Nucl. Phys. B **838**, 136 (2010). doi:[10.1016/j.nuclphysb.2010.05.008](https://doi.org/10.1016/j.nuclphysb.2010.05.008), arXiv:1002.4407
39. M. Botje et al., The PDF4LHC Working Group interim recommendations (2011). arXiv:1101.0538
40. G. Miu, T. Sjöstrand, W production in an improved parton-shower approach. Phys. Lett. B **449**, 313 (1999). doi:[10.1016/S0370-2693\(99\)00068-4](https://doi.org/10.1016/S0370-2693(99)00068-4)
41. K. Nakamura et al. (Particle Data Group), Review of particle physics. J. Phys. G **37**, 075021 (2010). doi:[10.1088/0954-3899/37/7A/075021](https://doi.org/10.1088/0954-3899/37/7A/075021)
42. M. Matchev, R. Remington, Updated templates for the interpretation of LHC results on supersymmetry in the context of mSUGRA (2012). arXiv:1202.6580
43. M. Dine, W. Fishler, A phenomenological model of particle physics based on supersymmetry. Phys. Lett. B **110**, 227 (1982). doi:[10.1016/0370-2693\(82\)91241-2](https://doi.org/10.1016/0370-2693(82)91241-2)
44. C.R. Nappi, B.A. Ovrut, Supersymmetric extension of the $SU(3) \times SU(2) \times U(1)$ model. Phys. Lett. B **113**, 175 (1982). doi:[10.1016/0370-2693\(82\)90418-X](https://doi.org/10.1016/0370-2693(82)90418-X)
45. L. Alvarez-Gaume, M. Claudson, M.B. Wise, Low-energy supersymmetry. Nucl. Phys. B **207**, 96 (1982). doi:[10.1016/0550-3213\(82\)90138-9](https://doi.org/10.1016/0550-3213(82)90138-9)

The CMS Collaboration

Yerevan Physics Institute, Yerevan, Armenia

S. Chatrchyan, V. Khachatryan, A.M. Sirunyan, A. Tumasyan

Institut für Hochenergiephysik der OeAW, Wien, Austria

W. Adam, E. Aguiló, T. Bergauer, M. Dragicevic, J. Erö, C. Fabjan¹, M. Friedl, R. Frühwirth¹, V.M. Ghete, J. Hammer, N. Hörmann, J. Hrubec, M. Jeitler¹, W. Kiesenhofer, V. Knünz, M. Krammer¹, I. Krätschmer, D. Liko, I. Mikulec, M. Pernicka[†], B. Rahbaran, C. Rohringer, H. Rohringer, R. Schöfbeck, J. Strauss, A. Taurok, W. Waltenberger, G. Walzel, E. Widl, C.-E. Wulz¹

National Centre for Particle and High Energy Physics, Minsk, Belarus

V. Mossolov, N. Shumeiko, J. Suarez Gonzalez

Universiteit Antwerpen, Antwerpen, Belgium

M. Bansal, S. Bansal, T. Cornelis, E.A. De Wolf, X. Janssen, S. Luyckx, L. Mucibello, S. Ochesanu, B. Roland, R. Rougny, M. Selvaggi, Z. Staykova, H. Van Haevermaet, P. Van Mechelen, N. Van Remortel, A. Van Spilbeeck

Vrije Universiteit Brussel, Brussel, Belgium

F. Blekman, S. Blyweert, J. D'Hondt, R. Gonzalez Suarez, A. Kalogeropoulos, M. Maes, A. Olbrechts, W. Van Doninck, P. Van Mulders, G.P. Van Onsem, I. Villella

Université Libre de Bruxelles, Bruxelles, Belgium

B. Clerbaux, G. De Lentdecker, V. Dero, A.P.R. Gay, T. Hreus, A. Léonard, P.E. Marage, A. Mohammadi, T. Reis, L. Thomas, G. Vander Marcken, C. Vander Velde, P. Vanlaer, J. Wang

Ghent University, Ghent, Belgium

V. Adler, K. Beernaert, A. Cimmino, S. Costantini, G. Garcia, M. Grunewald, B. Klein, J. Lellouch, A. Marinov, J. Mccartin, A.A. Ocampo Rios, D. Ryckbosch, N. Strobbe, F. Thyssen, M. Tytgat, P. Verwilligen, S. Walsh, E. Yazgan, N. Zaganidis

Université Catholique de Louvain, Louvain-la-Neuve, Belgium

S. Basegmez, G. Bruno, R. Castello, L. Ceard, C. Delaere, T. du Pree, D. Favart, L. Forthomme, A. Giannanco², J. Hollar, V. Lemaitre, J. Liao, O. Militaru, C. Nuttens, D. Pagano, A. Pin, K. Piotrkowski, N. Schul, J.M. Vizan Garcia

Université de Mons, Mons, Belgium

N. Beliy, T. Caebergs, E. Daubie, G.H. Hammad

Centro Brasileiro de Pesquisas Fisicas, Rio de Janeiro, Brazil

G.A. Alves, M. Correa Martins Junior, D. De Jesus Damiao, T. Martins, M.E. Pol, M.H.G. Souza

Universidade do Estado do Rio de Janeiro, Rio de Janeiro, Brazil

W.L. Aldá Júnior, W. Carvalho, A. Custódio, E.M. Da Costa, C. De Oliveira Martins, S. Fonseca De Souza, D. Matos Figueiredo, L. Mundim, H. Nogima, V. Oguri, W.L. Prado Da Silva, A. Santoro, L. Soares Jorge, A. Szajdor

Universidade Estadual Paulista^a, Universidade Federal do ABC^b, São Paulo, Brazil

T.S. Anjos^b, C.A. Bernardes^b, F.A. Dias^{a,3}, T.R. Fernandez Perez Tomei^a, E.M. Gregores^b, C. Lagana^a, F. Marinho^a, P.G. Mercadante^b, S.F. Novaes^a, S.S. Padula^a

Institute for Nuclear Research and Nuclear Energy, Sofia, Bulgaria

V. Genchev⁴, P. Iaydjiev⁴, S. Piperov, M. Rodozov, S. Stoykova, G. Sultanov, V. Tcholakov, R. Trayanov, M. Vutova

University of Sofia, Sofia, Bulgaria

A. Dimitrov, R. Hadjiiska, V. Kozhuharov, L. Litov, B. Pavlov, P. Petkov

Institute of High Energy Physics, Beijing, China

J.G. Bian, G.M. Chen, H.S. Chen, C.H. Jiang, D. Liang, S. Liang, X. Meng, J. Tao, J. Wang, X. Wang, Z. Wang, H. Xiao, M. Xu, J. Zang, Z. Zhang

State Key Laboratory of Nuclear Physics and Technology, Peking University, Beijing, China

C. Asawatangtrakuldee, Y. Ban, Y. Guo, W. Li, S. Liu, Y. Mao, S.J. Qian, H. Teng, D. Wang, L. Zhang, W. Zou

Universidad de Los Andes, Bogota, Colombia

C. Avila, J.P. Gomez, B. Gomez Moreno, A.F. Osorio Oliveros, J.C. Sanabria

Technical University of Split, Split, Croatia

N. Godinovic, D. Lelas, R. Plestina⁵, D. Polic, I. Puljak⁴

University of Split, Split, Croatia

Z. Antunovic, M. Kovac

Institute Rudjer Boskovic, Zagreb, Croatia

V. Brigljevic, S. Duric, K. Kadija, J. Luetic, S. Morovic

University of Cyprus, Nicosia, Cyprus

A. Attikis, M. Galanti, G. Mavromanolakis, J. Mousa, C. Nicolaou, F. Ptochos, P.A. Razis

Charles University, Prague, Czech Republic

M. Finger, M. Finger Jr.

Academy of Scientific Research and Technology of the Arab Republic of Egypt, Egyptian Network of High Energy Physics, Cairo, Egypt

Y. Assran⁶, S. Elgammal⁷, A. Ellithi Kamel⁸, M.A. Mahmoud⁹, A. Radi^{10,11}

National Institute of Chemical Physics and Biophysics, Tallinn, Estonia

M. Kadastik, M. Müntel, M. Raidal, L. Rebane, A. Tiko

Department of Physics, University of Helsinki, Helsinki, Finland

P. Eerola, G. Fedi, M. Voutilainen

Helsinki Institute of Physics, Helsinki, Finland

J. Hätkönen, A. Heikkinen, V. Karimäki, R. Kinnunen, M.J. Kortelainen, T. Lampén, K. Lassila-Perini, S. Lehti, T. Lindén, P. Luukka, T. Mäenpää, T. Peltola, E. Tuominen, J. Tuominiemi, E. Tuovinen, D. Ungaro, L. Wendland

Lappeenranta University of Technology, Lappeenranta, Finland

K. Banzuzi, A. Karjalainen, A. Korpela, T. Tuuva

DSM/IRFU, CEA/Saclay, Gif-sur-Yvette, France

M. Besancon, S. Choudhury, M. Dejardin, D. Denegri, B. Fabbro, J.L. Faure, F. Ferri, S. Ganjour, A. Givernaud, P. Gras, G. Hamel de Monchenault, P. Jarry, E. Locci, J. Malcles, L. Millischer, A. Nayak, J. Rander, A. Rosowsky, I. Shreyber, M. Titov

Laboratoire Leprince-Ringuet, Ecole Polytechnique, IN2P3-CNRS, Palaiseau, France

S. Baffioni, F. Baudette, L. Benhabib, L. Bianchini, M. Bluj¹², C. Broutin, P. Busson, C. Charlot, N. Daci, T. Dahms, L. Dobrzynski, R. Granier de Cassagnac, M. Haguenauer, P. Miné, C. Mironov, I.N. Naranjo, M. Nguyen, C. Ochando, P. Paganini, D. Sabes, R. Salerno, Y. Sirois, C. Veelken, A. Zabi

Institut Pluridisciplinaire Hubert Curien, Université de Strasbourg, Université de Haute Alsace Mulhouse, CNRS/IN2P3, Strasbourg, France

J.-L. Agram¹³, J. Andrea, D. Bloch, D. Bodin, J.-M. Brom, M. Cardaci, E.C. Chabert, C. Collard, E. Conte¹³, F. Drouhin¹³, C. Ferro, J.-C. Fontaine¹³, D. Gelé, U. Goerlach, P. Juillot, A.-C. Le Bihan, P. Van Hove

Centre de Calcul de l’Institut National de Physique Nucléaire et de Physique des Particules, CNRS/IN2P3, Villeurbanne, France

F. Fassi, D. Mercier

Université de Lyon, Université Claude Bernard Lyon 1, Institut de Physique Nucléaire de Lyon, CNRS-IN2P3, Villeurbanne, France

S. Beauceron, N. Beaupere, O. Bondu, G. Boudoul, J. Chasserat, R. Chierici⁴, D. Contardo, P. Depasse, H. El Mamouni, J. Fay, S. Gascon, M. Gouzevitch, B. Ille, T. Kurca, M. Lethuillier, L. Mirabito, S. Perries, L. Sgandurra, V. Sordini, Y. Tschudi, P. Verdier, S. Viret

Institute of High Energy Physics and Informatization, Tbilisi State University, Tbilisi, Georgia

Z. Tsamalaidze¹⁴

RWTH Aachen University, I. Physikalisches Institut, Aachen, Germany

G. Anagnostou, C. Autermann, S. Beranek, M. Edelhoff, L. Feld, N. Heracleous, O. Hindrichs, R. Jussen, K. Klein, J. Merz, A. Ostapchuk, A. Perieanu, F. Raupach, J. Sammet, S. Schael, D. Sprenger, H. Weber, B. Wittmer, V. Zhukov¹⁵

RWTH Aachen University, III. Physikalisches Institut A, Aachen, Germany

M. Ata, J. Caudron, E. Dietz-Laursonn, D. Duchardt, M. Erdmann, R. Fischer, A. Güth, T. Hebbeker, C. Heidemann, K. Hoepfner, D. Klingebiel, P. Kreuzer, M. Merschmeyer, A. Meyer, M. Olschewski, P. Papacz, H. Pieta, H. Reithler, S.A. Schmitz, L. Sonnenschein, J. Steggemann, D. Teyssier, M. Weber

RWTH Aachen University, III. Physikalisches Institut B, Aachen, Germany

M. Bontenackels, V. Cherepanov, Y. Erdogan, G. Flügge, H. Geenen, M. Geisler, W. Haj Ahmad, F. Hoehle, B. Kargoll, T. Kress, Y. Kuessel, J. Lingemann⁴, A. Nowack, L. Perchalla, O. Pooth, P. Sauerland, A. Stahl

Deutsches Elektronen-Synchrotron, Hamburg, Germany

M. Aldaya Martin, J. Behr, W. Behrenhoff, U. Behrens, M. Bergholz¹⁶, A. Bethani, K. Borras, A. Burgmeier, A. Cakir, L. Calligaris, A. Campbell, E. Castro, F. Costanza, D. Dammann, C. Diez Pardos, G. Eckerlin, D. Eckstein, G. Flucke, A. Geiser, I. Glushkov, P. Gunnellini, S. Habib, J. Hauk, G. Hellwig, H. Jung, M. Kasemann, P. Katsas, C. Kleinwort, H. Kluge, A. Knutsson, M. Krämer, D. Krücker, E. Kuznetsova, W. Lange, W. Lohmann¹⁶, B. Lutz, R. Mankel, I. Marfin, M. Marienfeld, I.-A. Melzer-Pellmann, A.B. Meyer, J. Mnich, A. Mussgiller, S. Naumann-Emme, O. Novgorodova, J. Olzem, H. Perrey, A. Petrukhin, D. Pitzl, A. Raspereza, P.M. Ribeiro Cipriano, C. Riedl, E. Ron, M. Rosin, J. Salfeld-Nebgen, R. Schmidt¹⁶, T. Schoerner-Sadenius, N. Sen, A. Spiridonov, M. Stein, R. Walsh, C. Wissing

University of Hamburg, Hamburg, Germany

V. Blobel, J. Draeger, H. Enderle, J. Erfle, U. Gebbert, M. Görner, T. Hermanns, R.S. Höing, K. Kaschube, G. Kaussen, H. Kirschenmann, R. Klanner, J. Lange, B. Mura, F. Nowak, T. Peiffer, N. Pietsch, D. Rathjens, C. Sander, H. Schettler, P. Schleper, E. Schlieckau, A. Schmidt, M. Schröder, T. Schum, M. Seidel, V. Sola, H. Stadie, G. Steinbrück, J. Thomsen, L. Vanelderen

Institut für Experimentelle Kernphysik, Karlsruhe, Germany

C. Barth, J. Berger, C. Böser, T. Chwalek, W. De Boer, A. Descroix, A. Dierlamm, M. Feindt, M. Guthoff⁴, C. Hackstein, F. Hartmann, T. Hauth⁴, M. Heinrich, H. Held, K.H. Hoffmann, S. Honc, I. Katkov¹⁵, J.R. Komaragiri, P. Lobelle Pardo, D. Martschei, S. Mueller, Th. Müller, M. Niegel, A. Nürnberg, O. Oberst, A. Oehler, J. Ott, G. Quast, K. Rabbertz, F. Ratnikov, N. Ratnikova, S. Röcker, A. Scheurer, F.-P. Schilling, G. Schott, H.J. Simonis, F.M. Stober, D. Troendle, R. Ulrich, J. Wagner-Kuhr, S. Wayand, T. Weiler, M. Zeise

Institute of Nuclear Physics “Demokritos”, Aghia Paraskevi, Greece

G. Daskalakis, T. Geralis, S. Kesisoglou, A. Kyriakis, D. Loukas, I. Manolakos, A. Markou, C. Markou, C. Mavrommatis, E. Ntomari

University of Athens, Athens, Greece

L. Gouskos, T.J. Mertzimekis, A. Panagiotou, N. Saoulidou

University of Ioánnina, Ioánnina, Greece

I. Evangelou, C. Foudas, P. Kokkas, N. Manthos, I. Papadopoulos, V. Patras

KFKI Research Institute for Particle and Nuclear Physics, Budapest, Hungary

G. Bencze, C. Hajdu, P. Hidas, D. Horvath¹⁷, F. Sikler, V. Veszpremi, G. Vesztergombi¹⁸

Institute of Nuclear Research ATOMKI, Debrecen, Hungary

N. Beni, S. Czellar, J. Molnar, J. Palinkas, Z. Szillasi

University of Debrecen, Debrecen, Hungary

J. Karancsi, P. Raics, Z.L. Trocsanyi, B. Ujvari

Panjab University, Chandigarh, India

S.B. Beri, V. Bhatnagar, N. Dhingra, R. Gupta, M. Kaur, M.Z. Mehta, N. Nishu, L.K. Saini, A. Sharma, J.B. Singh

University of Delhi, Delhi, India

Ashok Kumar, Arun Kumar, S. Ahuja, A. Bhardwaj, B.C. Choudhary, S. Malhotra, M. Naimuddin, K. Ranjan, V. Sharma, R.K. Shrivpuri

Saha Institute of Nuclear Physics, Kolkata, India

S. Banerjee, S. Bhattacharya, S. Dutta, B. Gomber, Sa. Jain, Sh. Jain, R. Khurana, S. Sarkar, M. Sharan

Bhabha Atomic Research Centre, Mumbai, India

A. Abdulsalam, R.K. Choudhury, D. Dutta, S. Kailas, V. Kumar, P. Mehta, A.K. Mohanty⁴, L.M. Pant, P. Shukla

Tata Institute of Fundamental Research - EHEP, Mumbai, India

T. Aziz, S. Ganguly, M. Guchait¹⁹, M. Maity²⁰, G. Majumder, K. Mazumdar, G.B. Mohanty, B. Parida, K. Sudhakar, N. Wickramage

Tata Institute of Fundamental Research - HEGR, Mumbai, India

S. Banerjee, S. Dugad

Institute for Research in Fundamental Sciences (IPM), Tehran, Iran

H. Arfaei²¹, H. Bakhshiansohi, S.M. Etesami²², A. Fahim²¹, M. Hashemi, H. Hesari, A. Jafari, M. Khakzad, M. Mohammadi Najafabadi, S. Pakhtinat Mehdiabadi, B. Safarzadeh²³, M. Zeinali

INFN Sezione di Bari^a, Università di Bari^b, Politecnico di Bari^c, Bari, Italy

M. Abbrescia^{a,b}, L. Barbone^{a,b}, C. Calabria^{a,b,4}, S.S. Chhibra^{a,b}, A. Colaleo^a, D. Creanza^{a,c}, N. De Filippis^{a,c,4}, M. De Palma^{a,b}, L. Fiore^a, G. Iaselli^{a,c}, L. Lusito^{a,b}, G. Maggi^{a,c}, M. Maggi^a, B. Marangelli^{a,b}, S. My^{a,c}, S. Nuzzo^{a,b}, N. Pacifico^{a,b}, A. Pompili^{a,b}, G. Pugliese^{a,c}, G. Selvaggi^{a,b}, L. Silvestris^a, G. Singh^{a,b}, R. Venditti^{a,b}, G. Zito

INFN Sezione di Bologna^a, Università di Bologna^b, Bologna, Italy

G. Abbiendi^a, A.C. Benvenuti^a, D. Bonacorsi^{a,b}, S. Braibant-Giacomelli^{a,b}, L. Brigliadori^{a,b}, P. Capiluppi^{a,b}, A. Castro^{a,b}, F.R. Cavallo^a, M. Cuffiani^{a,b}, G.M. Dallavalle^a, F. Fabbri^a, A. Fanfani^{a,b}, D. Fasanella^{a,b,4}, P. Giacomelli^a, C. Grandi^a, L. Guiducci^{a,b}, S. Marcellini^a, G. Masetti^a, M. Meneghelli^{a,b,4}, A. Montanari^a, F.L. Navarria^a, F. Odorici^a, A. Perrotta^a, F. Primavera^{a,b}, A.M. Rossi^{a,b}, T. Rovelli^{a,b}, G.P. Siroli^{a,b}, R. Travaglini^{a,b}

INFN Sezione di Catania^a, Università di Catania^b, Catania, Italy

S. Albergo^{a,b}, G. Cappello^{a,b}, M. Chiorboli^{a,b}, S. Costa^{a,b}, R. Potenza^{a,b}, A. Tricomi^{a,b}, C. Tuve^{a,b}

INFN Sezione di Firenze^a, Università di Firenze^b, Firenze, Italy

G. Barbagli^a, V. Ciulli^{a,b}, C. Civinini^a, R. D'Alessandro^{a,b}, E. Focardi^{a,b}, S. Frosali^{a,b}, E. Gallo^a, S. Gonzi^{a,b}, M. Meschini^a, S. Paoletti^a, G. Sguazzoni^a, A. Tropiano^a

INFN Laboratori Nazionali di Frascati, Frascati, Italy

L. Benussi, S. Bianco, S. Colafranceschi²⁴, F. Fabbri, D. Piccolo

INFN Sezione di Genova^a, Università di Genova^b, Genova, Italy

P. Fabbricatore^a, R. Musenich^a, S. Tosi^{a,b}

INFN Sezione di Milano-Bicocca^a, Università di Milano-Bicocca^b, Milano, Italy

A. Benaglia^{a,b}, F. De Guio^{a,b}, L. Di Matteo^{a,b,4}, S. Fiorendi^{a,b}, S. Gennai^{a,4}, A. Ghezzi^{a,b}, S. Malvezzi^a, R.A. Manzoni^{a,b}, A. Martelli^{a,b}, A. Massironi^{a,b,4}, D. Menasce^a, L. Moroni^a, M. Paganini^{a,b}, D. Pedrini^a, S. Ragazzi^{a,b}, N. Redaelli^a, S. Sala^a, T. Tabarelli de Fatis^{a,b}

INFN Sezione di Napoli^a, Università di Napoli 'Federico II'^b, Università della Basilicata (Potenza)^c, Università G. Marconi (Roma)^d, Napoli, Italy

S. Buontempo^a, C.A. Carrillo Montoya^a, N. Cavallo^{a,c}, A. De Cosa^{a,b,4}, O. Dogangun^{a,b}, F. Fabozzi^{a,c}, A.O.M. Iorio^{a,b}, L. Lista^a, S. Meola^{a,d,25}, M. Merola^a, P. Paolucci^{a,4}

INFN Sezione di Padova^a, Università di Padova^b, Università di Trento (Trento)^c, Padova, Italy

P. Azzi^a, N. Bacchetta^{a,4}, D. Bisello^{a,b}, A. Branca^{a,b,4}, R. Carlin^{a,b}, P. Checchia^a, T. Dorigo^a, F. Gasparini^{a,b}, U. Gasparini^{a,b}, A. Gozzelino^a, K. Kanishchev^{a,c}, S. Lacaprara^a, I. Lazzizzera^{a,c}, M. Margoni^{a,b}, A.T. Meneguzzo^{a,b}, J. Pazzini^{a,b}, N. Pozzobon^{a,b}, P. Ronchese^{a,b}, F. Simonetto^{a,b}, E. Torassa^a, M. Tosi^{a,b,4}, S. Vanini^{a,b}, P. Zotto^{a,b}, A. Zucchetta^{a,b}, G. Zumerle^{a,b}

INFN Sezione di Pavia^a, Università di Pavia^b, Pavia, Italy

M. Gabusi^{a,b}, S.P. Ratti^{a,b}, C. Riccardi^{a,b}, P. Torre^{a,b}, P. Vitulò^{a,b}

INFN Sezione di Perugia^a, Università di Perugia^b, Perugia, Italy

M. Biasini^{a,b}, G.M. Bilei^a, L. Fanò^{a,b}, P. Lariccia^{a,b}, A. Lucaroni^{a,b,4}, G. Mantovani^{a,b}, M. Menichelli^a, A. Nappi^{a,b,†}, F. Romeo^{a,b}, A. Saha^a, A. Santocchia^{a,b}, A. Spiezia^{a,b}, S. Taroni^{a,b}

INFN Sezione di Pisa^a, Università di Pisa^b, Scuola Normale Superiore di Pisa^c, Pisa, Italy

P. Azzurri^{a,c}, G. Bagliesi^a, J. Bernardini^a, T. Boccali^a, G. Broccolo^{a,c}, R. Castaldi^a, R.T. D'Agnolo^{a,c,4}, R. Dell'Orso^a, F. Fiori^{a,b,4}, L. Foà^{a,c}, A. Giassi^a, A. Kraan^a, F. Ligabue^{a,c}, T. Lomtadze^a, L. Martini^{a,26}, A. Messineo^{a,b}, F. Palla^a, A. Rizzi^{a,b}, A.T. Serban^{a,27}, P. Spagnolo^a, P. Squillaciotti^{a,4}, R. Tenchini^a, G. Tonelli^{a,b}, A. Venturi^a, P.G. Verdini^a

INFN Sezione di Roma^a, Università di Roma^b, Roma, Italy

L. Barone^{a,b}, F. Cavallari^a, D. Del Re^{a,b}, M. Diemoz^a, C. Fanelli^{a,b}, M. Grassi^{a,b,4}, E. Longo^{a,b}, P. Meridiani^{a,4}, F. Michelini^{a,b}, S. Nourbakhsh^{a,b}, G. Organtini^{a,b}, R. Paramatti^a, S. Rahatlou^{a,b}, M. Sigamani^a, L. Soffi^{a,b}

INFN Sezione di Torino^a, Università di Torino^b, Università del Piemonte Orientale (Novara)^c, Torino, Italy

N. Amapane^{a,b}, R. Arcidiacono^{a,c}, S. Argiro^{a,b}, M. Arneodo^{a,c}, C. Biino^a, N. Cartiglia^a, M. Costa^{a,b}, G. Dellacasa^a, N. Demaria^a, C. Mariotti^{a,4}, S. Maselli^a, E. Migliore^{a,b}, V. Monaco^{a,b}, M. Musich^{a,4}, M.M. Obertino^{a,c}, N. Pastrone^a, M. Pelliccioni^a, A. Potenza^{a,b}, A. Romero^{a,b}, R. Sacchi^{a,b}, A. Solano^{a,b}, A. Staiano^a, A. Vilela Pereira^a

INFN Sezione di Trieste^a, Università di Trieste^b, Trieste, Italy

S. Belforte^a, V. Candelise^{a,b}, M. Casarsa^a, F. Cossutti^a, G. Della Ricca^{a,b}, B. Gobbo^a, M. Marone^{a,b,4}, D. Montanino^{a,b,4}, A. Penzo^a, A. Schizzi^{a,b}

Kangwon National University, Chunchon, Korea

S.G. Heo, T.Y. Kim, S.K. Nam

Kyungpook National University, Daegu, Korea

S. Chang, D.H. Kim, G.N. Kim, D.J. Kong, H. Park, S.R. Ro, D.C. Son, T. Son

Chonnam National University, Institute for Universe and Elementary Particles, Kwangju, Korea

J.Y. Kim, Z.J. Kim, S. Song

Korea University, Seoul, Korea

S. Choi, D. Gyun, B. Hong, M. Jo, H. Kim, T.J. Kim, K.S. Lee, D.H. Moon, S.K. Park

University of Seoul, Seoul, Korea

M. Choi, J.H. Kim, C. Park, I.C. Park, S. Park, G. Ryu

Sungkyunkwan University, Suwon, Korea

Y. Cho, Y. Choi, Y.K. Choi, J. Goh, M.S. Kim, E. Kwon, B. Lee, J. Lee, S. Lee, H. Seo, I. Yu

Vilnius University, Vilnius, Lithuania

M.J. Bilinskas, I. Grigelionis, M. Janulis, A. Juodagalvis

Centro de Investigacion y de Estudios Avanzados del IPN, Mexico City, Mexico

H. Castilla-Valdez, E. De La Cruz-Burelo, I. Heredia-de La Cruz, R. Lopez-Fernandez, R. Magaña Villalba, J. Martínez-Ortega, A. Sanchez-Hernandez, L.M. Villasenor-Cendejas

Universidad Iberoamericana, Mexico City, Mexico

S. Carrillo Moreno, F. Vazquez Valencia

Benemerita Universidad Autonoma de Puebla, Puebla, Mexico

H.A. Salazar Ibarguen

Universidad Autónoma de San Luis Potosí, San Luis Potosí, Mexico

E. Casimiro Linares, A. Morelos Pineda, M.A. Reyes-Santos

University of Auckland, Auckland, New Zealand

D. Krofcheck

University of Canterbury, Christchurch, New Zealand

A.J. Bell, P.H. Butler, R. Doesburg, S. Reucroft, H. Silverwood

National Centre for Physics, Quaid-I-Azam University, Islamabad, Pakistan

M. Ahmad, M.H. Ansari, M.I. Asghar, H.R. Hoorani, S. Khalid, W.A. Khan, T. Khurshid, S. Qazi, M.A. Shah, M. Shoaib

National Centre for Nuclear Research, Swierk, Poland

H. Bialkowska, B. Boimska, T. Frueboes, R. Gokieli, M. Górska, M. Kazana, K. Nawrocki, K. Romanowska-Rybinska, M. Szleper, G. Wrochna, P. Zalewski

Institute of Experimental Physics, Faculty of Physics, University of Warsaw, Warsaw, Poland

G. Brona, K. Bunkowski, M. Cwiok, W. Dominik, K. Doroba, A. Kalinowski, M. Konecki, J. Krolikowski

Laboratório de Instrumentação e Física Experimental de Partículas, Lisboa, Portugal

N. Almeida, P. Bargassa, A. David, P. Faccioli, P.G. Ferreira Parracho, M. Gallinaro, J. Seixas, J. Varela, P. Vischia

Joint Institute for Nuclear Research, Dubna, Russia

P. Bunin, M. Gavrilenko, I. Golutvin, I. Gorbunov, V. Karjavin, V. Konoplyanikov, G. Kozlov, A. Lanev, A. Malakhov, P. Moisenz, V. Palichik, V. Perelygin, M. Savina, S. Shmatov, V. Smirnov, A. Volodko, A. Zarubin

Petersburg Nuclear Physics Institute, Gatchina (St. Petersburg), Russia

S. Evstyukhin, V. Golovtsov, Y. Ivanov, V. Kim, P. Levchenko, V. Murzin, V. Oreshkin, I. Smirnov, V. Sulimov, L. Uvarov, S. Vavilov, A. Vorobyev, An. Vorobyev

Institute for Nuclear Research, Moscow, Russia

Yu. Andreev, A. Dermenev, S. Glinenko, N. Golubev, M. Kirsanov, N. Krasnikov, V. Matveev, A. Pashenkov, D. Tlisov, A. Toropin

Institute for Theoretical and Experimental Physics, Moscow, Russia

V. Epshteyn, M. Erofeeva, V. Gavrilov, M. Kossov, N. Lychkovskaya, V. Popov, G. Safronov, S. Semenov, V. Stolin, E. Vlasov, A. Zhokin

P.N. Lebedev Physical Institute, Moscow, Russia

V. Andreev, M. Azarkin, I. Dremin, M. Kirakosyan, A. Leonidov, G. Mesyats, S.V. Rusakov, A. Vinogradov

Skobeltsyn Institute of Nuclear Physics, Lomonosov Moscow State University, Moscow, Russia

A. Belyaev, E. Boos, V. Bunichев, M. Dubinin³, L. Dudko, A. Ershov, A. Gribushin, V. Klyukhin, O. Kodolova, I. Loktin, A. Markina, S. Obraztsov, M. Perfilov, S. Petrushanko, A. Popov, L. Sarycheva[†], V. Savrin

State Research Center of Russian Federation, Institute for High Energy Physics, Protvino, Russia

I. Azhgirey, I. Bayshev, S. Bitioukov, V. Grishin⁴, V. Kachanov, D. Konstantinov, V. Krychkine, V. Petrov, R. Ryutin, A. Sobol, L. Tourtchanovitch, S. Troshin, N. Tyurin, A. Uzunian, A. Volkov

University of Belgrade, Faculty of Physics and Vinca Institute of Nuclear Sciences, Belgrade, Serbia

P. Adzic²⁸, M. Djordjevic, M. Ekmedzic, D. Krpic²⁸, J. Milosevic

Centro de Investigaciones Energéticas Medioambientales y Tecnológicas (CIEMAT), Madrid, Spain

M. Aguilar-Benitez, J. Alcaraz Maestre, P. Arce, C. Battilana, E. Calvo, M. Cerrada, M. Chamizo Llatas, N. Colino, B. De La Cruz, A. Delgado Peris, D. Domínguez Vázquez, C. Fernandez Bedoya, J.P. Fernández Ramos, A. Ferrando, J. Flix, M.C. Fouz, P. Garcia-Abia, O. Gonzalez Lopez, S. Goy Lopez, J.M. Hernandez, M.I. Josa, G. Merino, J. Puerta Pelayo, A. Quintario Olmeda, I. Redondo, L. Romero, J. Santaolalla, M.S. Soares, C. Willmott

Universidad Autónoma de Madrid, Madrid, Spain

C. Albajar, G. Codispoti, J.F. de Trocóniz

Universidad de Oviedo, Oviedo, Spain

H. Brun, J. Cuevas, J. Fernandez Menendez, S. Folgueras, I. Gonzalez Caballero, L. Lloret Iglesias, J. Piedra Gomez

Instituto de Física de Cantabria (IFCA), CSIC-Universidad de Cantabria, Santander, Spain

J.A. Brochero Cifuentes, I.J. Cabrillo, A. Calderon, S.H. Chuang, J. Duarte Campderros, M. Felcini²⁹, M. Fernandez, G. Gomez, J. Gonzalez Sanchez, A. Graziano, C. Jorda, A. Lopez Virto, J. Marco, R. Marco, C. Martinez Rivero, F. Matorras, F.J. Munoz Sanchez, T. Rodrigo, A.Y. Rodriguez-Marrero, A. Ruiz-Jimeno, L. Scodellaro, I. Vila, R. Vilar Cortabitarte

CERN, European Organization for Nuclear Research, Geneva, Switzerland

D. Abbaneo, E. Auffray, G. Auzinger, M. Bachtis, P. Baillon, A.H. Ball, D. Barney, J.F. Benitez, C. Bernet⁵, G. Bianchi, P. Bloch, A. Bocci, A. Bonato, C. Botta, H. Breuker, T. Camporesi, G. Cerminara, T. Christiansen, J.A. Coarasa Perez, D. D'Enterria, A. Dabrowski, A. De Roeck, S. Di Guida, M. Dobson, N. Dupont-Sagorin, A. Elliott-Peisert, B. Frisch, W. Funk, G. Georgiou, M. Giffels, D. Gigi, K. Gill, D. Giordano, M. Giunta, F. Glege, R. Gomez-Reino Garrido, P. Govoni, S. Gowdy, R. Guida, M. Hansen, P. Harris, C. Hartl, J. Harvey, B. Hegner, A. Hinzmamn, V. Innocente, P. Janot, K. Kaadze, E. Karavakis, K. Kousouris, P. Lecoq, Y.-J. Lee, P. Lenzi, C. Lourenço, N. Magini, T. Mäki, M. Malberti, L. Malgeri, M. Mannelli, L. Masetti, F. Meijers, S. Mersi, E. Meschi, R. Moser, M.U. Mozer, M. Mulders, P. Musella, E. Nesvold, T. Orimoto, L. Orsini, E. Palencia Cortezon, E. Perez, L. Perrozzi, A. Petrilli, A. Pfeiffer, M. Pierini, M. Pimiä, D. Piparo, G. Polese, L. Quertenmont, A. Racz, W. Reece, J. Rodrigues Antunes, G. Rolandi³⁰, C. Rovelli³¹, M. Rovere, H. Sakulin, F. Santanastasio, C. Schäfer, C. Schwick, I. Segoni, S. Sekmen, A. Sharma, P. Siegrist, P. Silva, M. Simon, P. Sphicas³², D. Spiga, A. Tsirou, G.I. Veres¹⁸, J.R. Vlimant, H.K. Wöhri, S.D. Worm³³, W.D. Zeuner

Paul Scherrer Institut, Villigen, Switzerland

W. Bertl, K. Deiters, W. Erdmann, K. Gabathuler, R. Horisberger, Q. Ingram, H.C. Kaestli, S. König, D. Kotlinski, U. Langenegger, F. Meier, D. Renker, T. Rohe, J. Sibille³⁴

Institute for Particle Physics, ETH Zurich, Zurich, Switzerland

L. Bäni, P. Bortignon, M.A. Buchmann, B. Casal, N. Chanon, A. Deisher, G. Dissertori, M. Dittmar, M. Donegà, M. Dünser, J. Eugster, K. Freudenreich, C. Grab, D. Hits, P. Lecomte, W. Lustermann, A.C. Marini, P. Martinez Ruiz del Arbol, N. Mohr, F. Moortgat, C. Nägeli³⁵, P. Nef, F. Nessi-Tedaldi, F. Pandolfi, L. Pape, F. Pauss, M. Peruzzi, F.J. Ronga, M. Rossini, L. Sala, A.K. Sanchez, A. Starodumov³⁶, B. Stieger, M. Takahashi, L. Tauscher[†], A. Thea, K. Theofilatos, D. Treille, C. Urscheler, R. Wallny, H.A. Weber, L. Wehrli

Universität Zürich, Zurich, Switzerland

C. Amsler, V. Chiochia, S. De Visscher, C. Favaro, M. Ivova Rikova, B. Millan Mejias, P. Otiougova, P. Robmann, H. Snoek, S. Tupputi, M. Verzetti

National Central University, Chung-Li, Taiwan

Y.H. Chang, K.H. Chen, C.M. Kuo, S.W. Li, W. Lin, Z.K. Liu, Y.J. Lu, D. Mekterovic, A.P. Singh, R. Volpe, S.S. Yu

National Taiwan University (NTU), Taipei, Taiwan

P. Bartalini, P. Chang, Y.H. Chang, Y.W. Chang, Y. Chao, K.F. Chen, C. Dietz, U. Grundler, W.-S. Hou, Y. Hsiung, K.Y. Kao, Y.J. Lei, R.-S. Lu, D. Majumder, E. Petrakou, X. Shi, J.G. Shiu, Y.M. Tzeng, X. Wan, M. Wang

Chulalongkorn University, Bangkok, Thailand

B. Asavabhiphop, N. Srimanobhas

Cukurova University, Adana, Turkey

A. Adiguzel, M.N. Bakirci³⁷, S. Cerci³⁸, C. Dozen, I. Dumanoglu, E. Eskut, S. Girgis, G. Gokbulut, E. Gurpinar, I. Hos, E.E. Kangal, T. Karaman, G. Karapinar³⁹, A. Kayis Topaksu, G. Onengut, K. Ozdemir, S. Ozturk⁴⁰, A. Polatoz, K. Sogut⁴¹, D. Sunar Cerci³⁸, B. Tali³⁸, H. Topaklı³⁷, L.N. Vergili, M. Vergili

Middle East Technical University, Physics Department, Ankara, Turkey

I.V. Akin, T. Aliev, B. Bilin, S. Bilmis, M. Deniz, H. Gamsizkan, A.M. Guler, K. Ocalan, A. Ozpineci, M. Serin, R. Sever, U.E. Surat, M. Yalvac, E. Yildirim, M. Zeyrek

Bogazici University, Istanbul, Turkey

E. Gülmез, B. Isildak⁴², M. Kaya⁴³, O. Kaya⁴³, S. Ozkorucuklu⁴⁴, N. Sonmez⁴⁵

Istanbul Technical University, Istanbul, Turkey

K. Cankocak

National Scientific Center, Kharkov Institute of Physics and Technology, Kharkov, Ukraine

L. Levchuk

University of Bristol, Bristol, United Kingdom

F. Bostock, J.J. Brooke, E. Clement, D. Cussans, H. Flacher, R. Frazier, J. Goldstein, M. Grimes, G.P. Heath, H.F. Heath, L. Kreczko, S. Metson, D.M. Newbold³³, K. Nirunpong, A. Poll, S. Senkin, V.J. Smith, T. Williams

Rutherford Appleton Laboratory, Didcot, United Kingdom

L. Basso⁴⁶, K.W. Bell, A. Belyaev⁴⁶, C. Brew, R.M. Brown, D.J.A. Cockerill, J.A. Coughlan, K. Harder, S. Harper, J. Jackson, B.W. Kennedy, E. Olaiya, D. Petty, B.C. Radburn-Smith, C.H. Shepherd-Themistocleous, I.R. Tomalin, W.J. Womersley

Imperial College, London, United Kingdom

R. Bainbridge, G. Ball, R. Beuselinck, O. Buchmuller, D. Colling, N. Cripps, M. Cutajar, P. Dauncey, G. Davies, M. Della Negra, W. Ferguson, J. Fulcher, A. Gilbert, A. Guneratne Bryer, G. Hall, Z. Hatherell, J. Hays, G. Iles, M. Jarvis, G. Karapostoli, L. Lyons, A.-M. Magnan, J. Marrouche, B. Mathias, R. Nandi, J. Nash, A. Nikitenko³⁶, A. Papageorgiou, J. Pela, M. Pesaresi, K. Petridis, M. Pioppi⁴⁷, D.M. Raymond, S. Rogerson, A. Rose, M.J. Ryan, C. Seez, P. Sharp[†], A. Sparrow, M. Stoye, A. Tapper, M. Vazquez Acosta, T. Virdee, S. Wakefield, N. Wardle, T. Whyntie

Brunel University, Uxbridge, United Kingdom

M. Chadwick, J.E. Cole, P.R. Hobson, A. Khan, P. Kyberd, D. Leggat, D. Leslie, W. Martin, I.D. Reid, P. Symonds, L. Teodorescu, M. Turner

Baylor University, Waco, USA

K. Hatakeyama, H. Liu, T. Scarborough

The University of Alabama, Tuscaloosa, USA

O. Charaf, C. Henderson, P. Rumerio

Boston University, Boston, USA

A. Avetisyan, T. Bose, C. Fantasia, A. Heister, P. Lawson, D. Lazic, J. Rohlf, D. Sperka, J. St. John, L. Sulak

Brown University, Providence, USA

J. Alimena, S. Bhattacharya, D. Cutts, A. Ferapontov, U. Heintz, S. Jabeen, G. Kukartsev, E. Laird, G. Landsberg, M. Luk, M. Narain, D. Nguyen, M. Segala, T. Sinthuprasith, T. Speer, K.V. Tsang

University of California, Davis, USA

R. Breedon, G. Breto, M. Calderon De La Barca Sanchez, S. Chauhan, M. Chertok, J. Conway, R. Conway, P.T. Cox, J. Dolen, R. Erbacher, M. Gardner, R. Houtz, W. Ko, A. Kopecky, R. Lander, T. Miceli, D. Pellett, F. Ricci-Tam, B. Rutherford, M. Searle, J. Smith, M. Squires, M. Tripathi, R. Vasquez Sierra

University of California, Los Angeles, USA

V. Andreev, D. Cline, R. Cousins, J. Duris, S. Erhan, P. Everaerts, C. Farrell, J. Hauser, M. Ignatenko, C. Jarvis, C. Plager, G. Rakness, P. Schlein[†], P. Traczyk, V. Valuev, M. Weber

University of California, Riverside, Riverside, USA

J. Babb, R. Clare, M.E. Dinardo, J. Ellison, J.W. Gary, F. Giordano, G. Hanson, G.Y. Jeng⁴⁸, H. Liu, O.R. Long, A. Luthra, H. Nguyen, S. Paramesvaran, J. Sturdy, S. Sumowidagdo, R. Wilken, S. Wimpenny

University of California, San Diego, La Jolla, USA

W. Andrews, J.G. Branson, G.B. Cerati, S. Cittolin, D. Evans, F. Golf, A. Holzner, R. Kelley, M. Lebourgeois, J. Letts, I. Macneill, B. Mangano, S. Padhi, C. Palmer, G. Petrucciani, M. Pieri, M. Sani, V. Sharma, S. Simon, E. Sudano, M. Tadel, Y. Tu, A. Vartak, S. Wasserbaech⁴⁹, F. Würthwein, A. Yagil, J. Yoo

University of California, Santa Barbara, Santa Barbara, USA

D. Barge, R. Bellan, C. Campagnari, M. D'Alfonso, T. Danielson, K. Flowers, P. Geffert, J. Incandela, C. Justus, P. Kalavase, S.A. Koay, D. Kovalskyi, V. Krutelyov, S. Lowette, N. Mccoll, V. Pavlunin, F. Rebassoo, J. Ribnik, J. Richman, R. Rossin, D. Stuart, W. To, C. West

California Institute of Technology, Pasadena, USA

A. Apresyan, A. Bornheim, Y. Chen, E. Di Marco, J. Duarte, M. Gataullin, Y. Ma, A. Mott, H.B. Newman, C. Rogan, M. Spiropulu, V. Timciuc, J. Veverka, R. Wilkinson, S. Xie, Y. Yang, R.Y. Zhu

Carnegie Mellon University, Pittsburgh, USA

B. Akgun, V. Azzolini, A. Calamba, R. Carroll, T. Ferguson, Y. Iiyama, D.W. Jang, Y.F. Liu, M. Paulini, H. Vogel, I. Vorobiev

University of Colorado at Boulder, Boulder, USA

J.P. Cumalat, B.R. Drell, C.J. Edelmaier, W.T. Ford, A. Gaz, B. Heyburn, E. Luiggi Lopez, J.G. Smith, K. Stenson, K.A. Ulmer, S.R. Wagner

Cornell University, Ithaca, USA

J. Alexander, A. Chatterjee, N. Eggert, L.K. Gibbons, B. Heltsley, A. Khukhunaishvili, B. Kreis, N. Mirman, G. Nicolas Kaufman, J.R. Patterson, A. Ryd, E. Salvati, W. Sun, W.D. Teo, J. Thom, J. Thompson, J. Tucker, J. Vaughan, Y. Weng, L. Winstrom, P. Wittich

Fairfield University, Fairfield, USA

D. Winn

Fermi National Accelerator Laboratory, Batavia, USA

S. Abdullin, M. Albrow, J. Anderson, L.A.T. Bauerick, A. Beretvas, J. Berryhill, P.C. Bhat, I. Bloch, K. Burkett, J.N. Butler, V. Chetluru, H.W.K. Cheung, F. Chlebana, V.D. Elvira, I. Fisk, J. Freeman, Y. Gao, D. Green, O. Gutsche, J. Hanlon, R.M. Harris, J. Hirschauer, B. Hooberman, S. Jindariani, M. Johnson, U. Joshi, B. Kilminster, B. Klima, S. Kunori, S. Kwan, C. Leonidopoulos, J. Linacre, D. Lincoln, R. Lipton, J. Lykken, K. Maeshima, J.M. Marraffino, S. Maruyama, D. Mason, P. McBride, K. Mishra, S. Mrenna, Y. Musienko⁵⁰, C. Newman-Holmes, V. O'Dell, O. Prokofyev, E. Sexton-Kennedy, S. Sharma, W.J. Spalding, L. Spiegel, P. Tan, L. Taylor, S. Tkaczyk, N.V. Tran, L. Uplegger, E.W. Vaandering, R. Vidal, J. Whitmore, W. Wu, F. Yang, F. Yumiceva, J.C. Yun

University of Florida, Gainesville, USA

D. Acosta, P. Avery, D. Bourilkov, M. Chen, T. Cheng, S. Das, M. De Gruttola, G.P. Di Giovanni, D. Dobur, A. Drozdetskiy, R.D. Field, M. Fisher, Y. Fu, I.K. Furic, J. Gartner, J. Hugon, B. Kim, J. Konigsberg, A. Korytov, A. Kropivnitskaya, T. Kypreos, J.F. Low, K. Matchev, P. Milenovic⁵¹, G. Mitselmakher, L. Muniz, M. Park, R. Remington, A. Rinkevicius, P. Sellers, N. Skhirtladze, M. Snowball, J. Yelton, M. Zakaria

Florida International University, Miami, USA

V. Gaultney, S. Hewamanage, L.M. Lebolo, S. Linn, P. Markowitz, G. Martinez, J.L. Rodriguez

Florida State University, Tallahassee, USA

T. Adams, A. Askew, J. Bochenek, J. Chen, B. Diamond, S.V. Gleyzer, J. Haas, S. Hagopian, V. Hagopian, M. Jenkins, K.F. Johnson, H. Prosper, V. Veeraraghavan, M. Weinberg

Florida Institute of Technology, Melbourne, USA

M.M. Baarmand, B. Dorney, M. Hohlmann, H. Kalakhety, I. Vodopiyanov

University of Illinois at Chicago (UIC), Chicago, USA

M.R. Adams, I.M. Anghel, L. Apanasevich, Y. Bai, V.E. Bazterra, R.R. Betts, I. Bucinskaite, J. Callner, R. Cavanaugh, O. Evdokimov, L. Gauthier, C.E. Gerber, D.J. Hofman, S. Khalatyan, F. Lacroix, M. Malek, C. O'Brien, C. Silkworth, D. Strom, P. Turner, N. Varelas

The University of Iowa, Iowa City, USA

U. Akgun, E.A. Albayrak, B. Bilki⁵², W. Clarida, F. Duru, S. Griffiths, J.-P. Merlo, H. Mermerkaya⁵³, A. Mestvirishvili, A. Moeller, J. Nachtman, C.R. Newsom, E. Norbeck, Y. Onel, F. Ozok⁵⁴, S. Sen, E. Tiras, J. Wetzel, T. Yetkin, K. Yi

Johns Hopkins University, Baltimore, USA

B.A. Barnett, B. Blumenfeld, S. Bolognesi, D. Fehling, G. Giurgiu, A.V. Gritsan, Z.J. Guo, G. Hu, P. Maksimovic, S. Rapoport, M. Swartz, A. Whitbeck

The University of Kansas, Lawrence, USA

P. Baringer, A. Bean, G. Benelli, R.P. Kenny III, M. Murray, D. Noonan, S. Sanders, R. Stringer, G. Tinti, J.S. Wood, V. Zhukova

Kansas State University, Manhattan, USA

A.F. Barfuss, T. Bolton, I. Chakaberia, A. Ivanov, S. Khalil, M. Makouski, Y. Maravin, S. Shrestha, I. Svintradze

Lawrence Livermore National Laboratory, Livermore, USA

J. Gronberg, D. Lange, D. Wright

University of Maryland, College Park, USA

A. Baden, M. Boutemeur, B. Calvert, S.C. Eno, J.A. Gomez, N.J. Hadley, R.G. Kellogg, M. Kirn, T. Kolberg, Y. Lu, M. Marionneau, A.C. Mignerey, K. Pedro, A. Peterman, A. Skuja, J. Temple, M.B. Tonjes, S.C. Tonwar, E. Twedt

Massachusetts Institute of Technology, Cambridge, USA

A. Apyan, G. Bauer, J. Bendavid, W. Busza, E. Butz, I.A. Cali, M. Chan, V. Dutta, G. Gomez Ceballos, M. Goncharov, K.A. Hahn, Y. Kim, M. Klute, K. Krajczar⁵⁵, W. Li, P.D. Luckey, T. Ma, S. Nahm, C. Paus, D. Ralph, C. Roland, G. Roland, M. Rudolph, G.S.F. Stephans, F. Stöckli, K. Sumorok, K. Sung, D. Velicanu, E.A. Wenger, R. Wolf, B. Wyslouch, M. Yang, Y. Yilmaz, A.S. Yoon, M. Zanetti

University of Minnesota, Minneapolis, USA

S.I. Cooper, B. Dahmes, A. De Benedetti, G. Franzoni, A. Gude, S.C. Kao, K. Klapoetke, Y. Kubota, J. Mans, N. Pastika, R. Rusack, M. Sasseville, A. Singovsky, N. Tambe, J. Turkewitz

University of Mississippi, Oxford, USA

L.M. Cremaldi, R. Kroeger, L. Perera, R. Rahmat, D.A. Sanders

University of Nebraska-Lincoln, Lincoln, USA

E. Avdeeva, K. Bloom, S. Bose, J. Butt, D.R. Claes, A. Dominguez, M. Eads, J. Keller, I. Kravchenko, J. Lazo-Flores, H. Malbouisson, S. Malik, G.R. Snow

State University of New York at Buffalo, Buffalo, USA

U. Baur, A. Godshalk, I. Iashvili, S. Jain, A. Kharchilava, A. Kumar, S.P. Shipkowski, K. Smith

Northeastern University, Boston, USA

G. Alverson, E. Barberis, D. Baumgartel, M. Chasco, J. Haley, D. Nash, D. Trocino, D. Wood, J. Zhang

Northwestern University, Evanston, USA

A. Anastassov, A. Kubik, N. Mucia, N. Odell, R.A. Ofierzynski, B. Pollack, A. Pozdnyakov, M. Schmitt, S. Stoynev, M. Velasco, S. Won

University of Notre Dame, Notre Dame, USA

L. Antonelli, D. Berry, A. Brinkerhoff, M. Hildreth, C. Jessop, D.J. Karmgard, J. Kolb, K. Lannon, W. Luo, S. Lynch, N. Marinelli, D.M. Morse, T. Pearson, M. Planer, R. Ruchti, J. Slaunwhite, N. Valls, M. Wayne, M. Wolf

The Ohio State University, Columbus, USA

B. Bylsma, L.S. Durkin, C. Hill, R. Hughes, K. Kotov, T.Y. Ling, D. Puigh, M. Rodenburg, C. Vuosalo, G. Williams, B.L. Winer

Princeton University, Princeton, USA

N. Adam, E. Berry, P. Elmer, D. Gerbaudo, V. Halyo, P. Hebda, J. Hegeman, A. Hunt, P. Jindal, D. Lopes Pegna, P. Lujan, D. Marlow, T. Medvedeva, M. Mooney, J. Olsen, P. Piroué, X. Quan, A. Raval, B. Safdi, H. Saka, D. Stickland, C. Tully, J.S. Werner, A. Zuranski

University of Puerto Rico, Mayaguez, USA

J.G. Acosta, E. Brownson, X.T. Huang, A. Lopez, H. Mendez, S. Oliveros, J.E. Ramirez Vargas, A. Zatserklyaniy

Purdue University, West Lafayette, USA

E. Alagoz, V.E. Barnes, D. Benedetti, G. Bolla, D. Bortoletto, M. De Mattia, A. Everett, Z. Hu, M. Jones, O. Koybasi, M. Kress, A.T. Laasanen, N. Leonardo, V. Maroussov, P. Merkel, D.H. Miller, N. Neumeister, I. Shipsey, D. Silvers, A. Svyatkovskiy, M. Vidal Marono, H.D. Yoo, J. Zablocki, Y. Zheng

Purdue University Calumet, Hammond, USA

S. Guragain, N. Parashar

Rice University, Houston, USA

A. Adair, C. Boulahouache, K.M. Ecklund, F.J.M. Geurts, B.P. Padley, R. Redjimi, J. Roberts, J. Zabel

University of Rochester, Rochester, USA

B. Betchart, A. Bodek, Y.S. Chung, R. Covarelli, P. de Barbaro, R. Demina, Y. Eshaq, T. Ferbel, A. Garcia-Bellido, P. Goldenzweig, J. Han, A. Harel, D.C. Miner, D. Vishnevskiy, M. Zielinski

The Rockefeller University, New York, USA

A. Bhatti, R. Ciesielski, L. Demortier, K. Goulian, G. Lungu, S. Malik, C. Mesropian

Rutgers, the State University of New Jersey, Piscataway, USA

S. Arora, A. Barker, J.P. Chou, C. Contreras-Campana, E. Contreras-Campana, D. Duggan, D. Ferencek, Y. Gershtein, R. Gray, E. Halkiadakis, D. Hidas, A. Lath, S. Panwalkar, M. Park, R. Patel, V. Rekovic, J. Robles, K. Rose, S. Salur, S. Schnetzer, C. Seitz, S. Somalwar, R. Stone, S. Thomas

University of Tennessee, Knoxville, USA

G. Cerizza, M. Hollingsworth, S. Spanier, Z.C. Yang, A. York

Texas A&M University, College Station, USA

R. Eusebi, W. Flanagan, J. Gilmore, T. Kamon⁵⁶, V. Khotilovich, R. Montalvo, I. Osipenkov, Y. Pakhotin, A. Perloff, J. Roe, A. Safonov, T. Sakuma, S. Sengupta, I. Suarez, A. Tatarinov, D. Toback

Texas Tech University, Lubbock, USA

N. Akchurin, J. Damgov, C. Dragoiu, P.R. Dudero, C. Jeong, K. Kovitanggoon, S.W. Lee, T. Libeiro, Y. Roh, I. Volobouev

Vanderbilt University, Nashville, USA

E. Appelt, A.G. Delannoy, C. Florez, S. Greene, A. Gurrola, W. Johns, C. Johnston, P. Kurt, C. Maguire, A. Melo, M. Sharma, P. Sheldon, B. Snook, S. Tuo, J. Velkovska

University of Virginia, Charlottesville, USA

M.W. Arenton, M. Balazs, S. Boutle, B. Cox, B. Francis, J. Goodell, R. Hirosky, A. Ledovskoy, C. Lin, C. Neu, J. Wood, R. Yohay

Wayne State University, Detroit, USA

S. Gollapinni, R. Harr, P.E. Karchin, C. Kottachchi Kankamamge Don, P. Lamichhane, A. Sakharov

University of Wisconsin, Madison, USA

M. Anderson, D.A. Belknap, L. Borrello, D. Carlsmith, M. Cepeda, S. Dasu, E. Friis, L. Gray, K.S. Grogg, M. Grothe, R. Hall-Wilton, M. Herndon, A. Hervé, P. Klabbers, J. Klukas, A. Lanaro, C. Lazaridis, J. Leonard, R. Loveless, A. Mohapatra, I. Ojalvo, F. Palmonari, G.A. Pierro, I. Ross, A. Savin, W.H. Smith, J. Swanson

†: Deceased

- 1: Also at Vienna University of Technology, Vienna, Austria
- 2: Also at National Institute of Chemical Physics and Biophysics, Tallinn, Estonia
- 3: Also at California Institute of Technology, Pasadena, USA
- 4: Also at CERN, European Organization for Nuclear Research, Geneva, Switzerland
- 5: Also at Laboratoire Leprince-Ringuet, Ecole Polytechnique, IN2P3-CNRS, Palaiseau, France
- 6: Also at Suez Canal University, Suez, Egypt
- 7: Also at Zewail City of Science and Technology, Zewail, Egypt
- 8: Also at Cairo University, Cairo, Egypt
- 9: Also at Fayoum University, El-Fayoum, Egypt
- 10: Also at British University in Egypt, Cairo, Egypt
- 11: Now at Ain Shams University, Cairo, Egypt
- 12: Also at National Centre for Nuclear Research, Swierk, Poland
- 13: Also at Université de Haute Alsace, Mulhouse, France
- 14: Now at Joint Institute for Nuclear Research, Dubna, Russia
- 15: Also at Skobeltsyn Institute of Nuclear Physics, Lomonosov Moscow State University, Moscow, Russia
- 16: Also at Brandenburg University of Technology, Cottbus, Germany
- 17: Also at Institute of Nuclear Research ATOMKI, Debrecen, Hungary
- 18: Also at Eötvös Loránd University, Budapest, Hungary
- 19: Also at Tata Institute of Fundamental Research - HECR, Mumbai, India
- 20: Also at University of Visva-Bharati, Santiniketan, India
- 21: Also at Sharif University of Technology, Tehran, Iran
- 22: Also at Isfahan University of Technology, Isfahan, Iran
- 23: Also at Plasma Physics Research Center, Science and Research Branch, Islamic Azad University, Tehran, Iran
- 24: Also at Facoltà Ingegneria, Università di Roma, Roma, Italy
- 25: Also at Università degli Studi Guglielmo Marconi, Roma, Italy
- 26: Also at Università degli Studi di Siena, Siena, Italy
- 27: Also at University of Bucharest, Faculty of Physics, Bucuresti-Magurele, Romania
- 28: Also at Faculty of Physics of University of Belgrade, Belgrade, Serbia
- 29: Also at University of California, Los Angeles, USA
- 30: Also at Scuola Normale e Sezione dell'INFN, Pisa, Italy
- 31: Also at INFN Sezione di Roma; Università di Roma, Roma, Italy
- 32: Also at University of Athens, Athens, Greece
- 33: Also at Rutherford Appleton Laboratory, Didcot, United Kingdom
- 34: Also at The University of Kansas, Lawrence, USA
- 35: Also at Paul Scherrer Institut, Villigen, Switzerland
- 36: Also at Institute for Theoretical and Experimental Physics, Moscow, Russia
- 37: Also at Gaziosmanpasa University, Tokat, Turkey
- 38: Also at Adiyaman University, Adiyaman, Turkey
- 39: Also at Izmir Institute of Technology, Izmir, Turkey
- 40: Also at The University of Iowa, Iowa City, USA
- 41: Also at Mersin University, Mersin, Turkey
- 42: Also at Ozyegin University, Istanbul, Turkey
- 43: Also at Kafkas University, Kars, Turkey
- 44: Also at Suleyman Demirel University, Isparta, Turkey
- 45: Also at Ege University, Izmir, Turkey
- 46: Also at School of Physics and Astronomy, University of Southampton, Southampton, United Kingdom
- 47: Also at INFN Sezione di Perugia; Università di Perugia, Perugia, Italy

- 48: Also at University of Sydney, Sydney, Australia
49: Also at Utah Valley University, Orem, USA
50: Also at Institute for Nuclear Research, Moscow, Russia
51: Also at University of Belgrade, Faculty of Physics and Vinca Institute of Nuclear Sciences, Belgrade, Serbia
52: Also at Argonne National Laboratory, Argonne, USA
53: Also at Erzincan University, Erzincan, Turkey
54: Also at Mimar Sinan University, Istanbul, Istanbul, Turkey
55: Also at KFKI Research Institute for Particle and Nuclear Physics, Budapest, Hungary
56: Also at Kyungpook National University, Daegu, Korea